Docket No. SA-542

Exhibit No. 15-A

NATIONAL TRANSPORTATION SAFETY BOARD

Washington, D.C.

Materials Laboratory Factual Report 18-049

(40 Pages)

NATIONAL TRANSPORTATION SAFETY BOARD
Office of Research and Engineering
Materials Laboratory Division
Washington, D.C. 20594

October 25, 2018

MATERIALS LABORATORY FACTUAL REPORT Report No. 18-049

A. ACCIDENT INFORMATION

Place	:	Philadelphia, Pennsylvania
Date	:	April 17, 2018
Vehicle	:	Boeing 737-700, N772SW
NTSB No.	:	DCA18MA142
Investigator	:	Pierre Scarfo, AS-40

B. COMPONENTS EXAMINED

Fan blades, fan blade shims, fan blade spacers, and fan blade platforms from the accident engine and four fan blades returned from field inspections.

C. DETAILS OF THE EXAMINATION

On April 17, 2018, at 1103 eastern daylight time, Southwest Airlines flight 1380, a Boeing 737-7H4, N772SW, experienced a left engine failure and loss of engine inlet and cowling during climb at about flight level 320. Fragments from the engine inlet and cowling struck the wing, fuselage, and one cabin window, resulting in a depressurization. The flight crew conducted an emergency descent and diverted into Philadelphia International Airport (KPHL), Philadelphia, PA. Of the 144 passengers and five crewmembers onboard, one passenger received fatal injuries and eight passengers received minor injuries. The airplane sustained substantial damage. The regularly scheduled domestic passenger flight was operating under 14 Code of Federal Regulations Part 121 from LaGuardia Airport (KLGA), Queens, New York, to Dallas Love Field (KDAL), Dallas, Texas.

An overall view of the left (number 1) engine after the accident is shown in figure 1. The engine inlet was fractured, and the forward portion of the inlet was missing. One of the 24 fan blades was fractured at the root, and the remaining blades showed impact damage. During engine operation, the fan blades rotate clockwise as viewed looking forward. The fan blades were numbered sequentially also in the clockwise direction in accordance with blade numbering instructions provided in the Boeing Aircraft Maintenance Manual[1] where the number 1 blade is located immediately above an offset hole on the fan disk. The fractured blade was blade 13 as indicated in figure 1.

[1] Aircraft Maintenance Manual, Boeing 737-600/700/800/900, The Boeing Company.

The installed engines were CFM International[2] CFM56-7B engines. A schematic drawing from the Aircraft Maintenance Manual shown in figure 2 illustrates the assembly of fan blades, shims, spacers, and platforms in the engine fan assembly. To facilitate examination of the fan blades from the number 1 engine, the fan blades, fan blade shims, fan blade spacers, and fan blade platforms were shipped to the NTSB Materials Laboratory for examination.

1. Fan Blade Construction

The fan blades are manufactured of a titanium alloy with 6 percent aluminum and 4 percent vanadium (commonly known as Ti-6-4). All titanium alloy surfaces of the blades are shot peened. The contact faces of the blade dovetail[3] are grit blasted and then coated with a copper alloy containing nickel and indium (Cu-Ni-In) applied by plasma spray. A baked dry-film lubricant of molybdenum disulfide is then applied to the exterior of the Cu-Ni-In coating. Another coating of molybdenum disulfide lubricant is sprayed on the surface before the blade is installed in the shim.

The shims are manufactured of alloy 718, a nickel-chromium-iron alloy. The contact faces on the exterior of the shims are also coated with a baked dry-film lubricant with additional lubrication applied by spray and by brush before installation in the fan disk slot during first assembly of the engine.

The fan blade spacers are manufactured of Ti-6-4 with an elastomer coating. The fan blade platforms between the blades are manufactured of an aluminum alloy and have elastomer seals on the sides in contact with the blades.

2. Service History

At the time of the accident, the number 1 engine had accumulated 67,040 hours time since new (TSN) and 40,569 flight cycles since new (CSN). Since the last shop visit in November 2012, the engine had accumulated 18,088 hours time since last shop visit (TSLSV) 10,712 flight cycles since last shop visit (CSLSV). All 24 fan blades from the number 1 engine experienced the same service history operating as a complete set with no blades within the set requiring replacement from the time of first installation on another engine in March 2001. The blades were manufactured as part 340-001-026-0 blades and were later changed to part number 340-001-038-0. The part number 340-001-026-0 blade, introduced in CFM International CFM56-7B Service Bulletin 72-0253, were manufactured with dovetail profiles modified from those of the original part number 340-001-022-0 blades to prevent premature spalling and wear damage of the Cu-Ni-In coating at the forward and aft ends of the contact faces. The blades had remained together as a set since they were first installed on another engine in March 2001 and were last installed on the accident engine at the last shop visit 18,089 hours TSLSV and 10,712 CSLSV. At the time of the accident, the blades had accumulated 55,471 hours TSN and 32,636 CSN.

[2] CFM International is a joint venture between GE Aviation and Safran Aircraft Engines.
[3] The dovetail is the root end of the blade where it is retained within a slot in the fan disk.

When the accident fan blades were installed in the other engines starting in 2001, the fan assembly design did not include fan blade shims. When the blades were installed in the accident engine in 2012, the blades were installed with fan blade shims since the disk in that engine was a newer design requiring installation of shims between the blades and the disk.

The fan blades were last overhauled before they were installed on the accident engine in September 2012. The blade overhaul process includes stripping the dovetail coating from the blades, fluorescent penetrant inspection (FPI), blend and repair of the airfoil leading edge as needed, shot peening of the entire blade, grit blasting the area of the dovetail to be coated, and coating the dovetail contact faces with the Cu-Ni-In coating followed by a cured dry-film lubricant. The blades had been overhauled one time prior in April 2004. The blades had 6,125 CSN at the time of the first overhaul.

Since 2004, engine records showed the fan blades received periodic lubrication. According to Aircraft Maintenance Manual procedures, the blades are removed from the disk and the components to be lubricated are cleaned. The blades are inspected for damage including nicks, dents, scratches, cracks, tears, and tip curl; and the dovetail is inspected for areas of missing coating from the contact face. Shims are also inspected for cracks, tears, punctures, scratches, nicks, dents, and distortion. Blades and shims with damage to the dry film lubricant are permitted to continue in service provided the fan blade set is lubricated before operating under revenue service. As part of the blade installation process, the fan blade spacers and shims, and the dovetail slots in the fan disk are all lubricated with Molykote D321 or Dow Corning 321 lubricant applied by spray or with Molykote G-n Plus or other lubricant meeting military standard MIL-L-8937 applied by brush. The thickness of the applied lubricant is specified to be 0.0003 inch to 0.0005 inch for the spray application or 0.004 inch to 0.008 inch for the brush application. The Boeing Maintenance Planning Document stated at the time of the accident that the blades and shims should be lubricated at intervals not to exceed 5,000 hours or 3,000 cycles, whichever occurs first.

On the accident engine, the fan blades and shims were lubricated 7 times since the November 2012 shop visit including the first installation after overhaul. The maintenance instructions provide the option to use spray or brush the lubricant onto the surface, and the operator chose to brush the lubricant on. The number of flight cycles between the last 7 fan blade lubrication applications (earliest to latest) were 1,392 cycles, 1,255 cycles, 1,265 cycles, 1,412 cycles, 98 cycles, 1,385 cycles, and 2,201 cycles. At the time of the accident, the fan blades had 1,704 cycles since the last lubrication.

3. Examination Process

Participants in the laboratory examination led by the NTSB included representatives from Southwest Airlines (airplane operator), GE Aviation (engine manufacturer), Safran Aircraft Engines (engine manufacturer), The Boeing Company (airplane manufacturer), UTC Aerospace Systems (engine inlet manufacturer), the Federal Aviation Administration (regulator), and the Bureau d'Enquêtes et d'Analyses pour la sécurité de l'aviation civile (French organization for aviation safety investigations).

Initially, the laboratory examination began at the NTSB Materials Laboratory in Washington, DC. In addition to continued work completed at the NTSB Materials Laboratory, work examining the submitted components during subsequent phases of the examination was completed at the GE Engineering Materials Systems in Evendale, Ohio, and the Safran Aircraft Engines Failure Analysis Laboratory in Moissy-Cramayel, France.[4]

The components submitted for examination were the fan blades, fan blade spacers, fan blade shims, and fan blade platforms from the number 1 engine. As of the time of this report, four additional fan blades with cracks detected from field inspections conducted after the accident were received by CFM International and were examined at either the GE Engineering Materials Systems (blades labeled M and O) or at the Safran Aircraft Engines Failure Analysis Laboratory (blades labeled N and P).[5] Results of the examination of those blades are described in the last section of this report.

Before the fan blades were transported to the NTSB Materials Laboratory, the intact blades were examined for crack indications using ultrasonic testing (UT). After arriving at the NTSB laboratory, the components were initially photographed and examined visually and under optical magnification. An initial examination of the fracture surface on blade 13 was also completed. After the initial examinations, the blade 13 piece was cleaned by application of acetate tape followed by use of an ultrasonic cleaner while submerged in a bath of acetone. Next, a detailed fractographic examination of the fracture surface from blade 13 was conducted including an examination using a scanning electron microscope (SEM). Metallographic sections were taken from the middle and near the trailing end of the dovetail contact area on blade 13. An SEM examination of the surface of blade 20 was also conducted to look for any evidence of crack initiation.

In the next stage of the examination, blades 1 through 12, 14 through 19, and 21 through 24 were sent to GE Aviation for non-destructive examination using fluorescent-penetrant inspection (FPI) and eddy-current inspection (ECI). In order to complete the FPI and ECI, the Cu-Ni-In coating was chemically stripped from the blades by soaking the dovetails in a bath of concentrated nitric acid. The blades were subsequently sent to the Safran Failure Analysis Laboratory for additional UT, FPI, and ECI and to complete a more detailed examination of features associated with ECI responses above a threshold level. Surfaces of the blade dovetails on blades 3, 12, 23, and 24 were also examined by SEM.

---

[4] Investigation Report CYA No. 68389, *CFM56-7B No.875134 SWA 22/24 Fan Blade Inspection*, Safran Aircraft Engines (September 17, 2018).

[5] Metallurgical Investigation Report Log No. FAL2018-18392, *Metallurgical Evaluation of a CFM56-7 Fan Blade from ESN 874-176 Operated by [domestic operator]*, GE Aviation (August 3, 2018).

Compte Rendu d'Examen CYA No. 68259, *CFM56-7B ESN 875774 – [foreign operator] Cracked Fan Blade P/N 340-001-020-0 -027-0 -037-0, S/N BB042335-D*, Safran Aircraft Engines (June 5, 2018).

Metallurgical Investigation Report Log No. FAL2018-18412, *Metallurgical Evaluation of a CFM56-7 Fan Blade from ESN 890-978 Operated by Southwest Airlines*, GE Aviation (August 3, 2018).

Investigation Report CYA No. 68392, *CFM56-7 SWA No.896763 Fan Blade P/N 340-001-027-0 – S/N DA934335-R Root Crack at Trailing Edge Concave Side*, Safran Aircraft Engines (July 20, 2018).

Residual stress was measured on selected blades from the accident engine. Tests were completed at Lambda Technologies Group (Cincinnati, Ohio) and at Safran Aircraft Engines.

4. Optical Examination

Overall views of the submitted components from the accident engine as received are shown in figures 3 and 4. The fan blade spacers and airfoil platforms are each shown below their respective blade as numbered at the bottom of each image. The shims for the intact blades had been removed earlier to complete the UT inspections, but the shims had been reinstalled on their respective dovetails as shown in figures 3 and 4. As installed on the airplane, the airfoil platforms are positioned between blades, and the platform number corresponds to the blade facing the convex side of the platform. Thus as numbered, the blade 13 platform was located between blade 13 and blade 14 and preceded blade 13 as the fan rotated. As indicated in figures 3 and 4, blade 14 preceded blade 13 in fan rotation, and blade 12 trailed blade 13.

a. Fan Blade 13

Blade 13 was fractured at the root and in the middle portion of the airfoil as shown in figure 5. The dovetail portion of the blade was retained within the fan disk, and the two airfoil pieces were recovered in the engine aft of the fan. The larger (inboard) airfoil piece had a fracture surface at the root end that mated to the fracture surface on the dovetail piece. To facilitate examination of the fracture surface, the shim was removed from the dovetail piece as shown in figure 5 by sliding it off the forward end of the dovetail piece. Each of the fan blade pieces were weighed, and the resulting measurements were 0.65 pound, 6.83 pounds, and 0.78 pound for the outboard airfoil piece, inboard airfoil piece, and dovetail piece, respectively. The total weight of the recovered blade pieces represented approximately 75% of the nominal weight (10.83 pounds) of a new fan blade.

The airfoils for the other 23 blades showed deformation, tearing, and fractures consistent with hard-body impacts such as from blade fragments. No evidence of feathers or blood was observed on the blades.

Following an initial visual examination of the blade 13 pieces, the fracture surface on the dovetail piece was cleaned using acetate replica tape that was first softened with acetone and pressed onto the surface. After the tape dried and hardened, the tape was removed, creating a replica of the fracture surface while also removing some of the deposits covering the fracture surface. The replica tape process was repeated, and then the fracture surface was submerged in acetone and cleaned using an ultrasonic cleaner.

An overall view of the fracture surface on the dovetail piece of blade 13 after cleaning is shown in figure 6. A portion of the fracture surface was relatively smoother with curving crack arrest lines, features consistent with fatigue. Fracture features emanated from an origin area centered approximately 0.57 inch from the leading-edge

face on the convex side of the blade as indicated with a bracket in figure 6. Ratchet marks[6] were observed in the origin area, consistent with multiple fatigue origins.

An overall view of the blade 13 dovetail piece and shim are shown in figure 7. The Cu-Ni-In coating was intact and appeared generally uniform in texture and color. The shim was largely intact with a small piece fractured and missing from the forward outboard corner. A closer view of the convex surface of the blade dovetail piece in the area of the fatigue origin is shown in figure 8. The fracture initiated approximately 0.036 inch outboard of the outboard edge[7] of the Cu-Ni-In coating (see figure 7).

A closer view of the fatigue region on the blade 13 piece is shown in figure 9. A dashed line in figure 9 represents a boundary of the fatigue region where well-defined curving crack arrest marks were observed. This region was 0.976 inch long axially at the blade surface and extended up to 0.263 inch deep. Beyond that region, fracture features were in a relatively flat plane with a curving boundary indicated with unlabeled arrows in figure 9. The flat-plane region defined by unlabeled arrows intersected the forward face and extended up to 2.232 inches axially and up to 0.483 inch deep. Beyond the boundary defined by unlabeled arrows, the fracture surface had a slightly different texture with prominent shear lips, features consistent with ductile overstress fracture.

Six distinct crack arrest lines were visible on the fracture surface as indicated in figure 10. The arrest lines are shown numbered starting with the arrest line closest to the origin. The maximum depths of the crack arrest lines were 0.037 inch, 0.068 inch, 0.094 inch, 0.143 inch, 0.187 inch, and 0.263 inch for arrest lines 1 to 6, respectively. Following the optical examination of the fracture surface, a detailed SEM examination of the surface was conducted as described later in this report.

b. Intact Fan Blades and Shims

The dovetails for the remaining blades were examined visually and using an optical stereomicroscope. The Cu-Ni-In coating on the dovetails overall had a mix of relatively rougher areas that were light gray to light gold in color mixed with areas that were smoother and dark gray to black in color. Deposits of gray lubricant were generally observed around the edges of the contact faces. The coating on many of the blades showed evidence of heavy sliding contact with sliding marks and deformation oriented in the radial direction. The blades also showed varying amounts of chipping and spalling of the Cu-Ni-In coating, leaving crater-like features in the contact faces of the dovetails. The disturbance to the Cu-Ni-In coating was predominantly at the forward and aft ends of the contact faces on the convex and concave sides of the dovetails, particularly in blades 18 through 24 and blades 1 through 4. Blades adjacent to the fractured blade also showed disturbances to the Cu-Ni-In coating with more sliding contact damage and fractured shims.

[6] A ratchet mark is a small step in the fracture surface formed when two adjacent fatigue cracks originate on slightly offset planes.
[7] Inboard and outboard reference positions relative to the fan disk's rotational axis where outboard is further from the axis in the radial direction.

Closer views of the dovetails for blades 12 and 20 are shown in figures 11 and 12 and are representative of blades with more extensive damage to the dovetail contact faces. Later examination of the corresponding shims revealed coating material adhered to the interior surfaces of the shim in areas where these crater-like features were observed. No evidence of cracks in other blades were detected during the optical examination.

Part numbers, serial numbers, moment weights, and commercial and government entity (CAGE) codes were marked on the root ends of the blades. A view of the root end of blade 13 is shown in figure 5.

All fan blade shims had a bridging piece across tangs at the forward side of the shim, consistent with a shim design introduced in 2008. Most of the shims were intact as shown in figures 3 and 4. The shim for blade 11 was cracked at the outboard edge of the contact face on the concave side of the shim. The shim for blade 12 was fractured along the inboard edge of the contact face on both sides of the shim. The pieces outboard of the fractures in shim 12 were missing.

The exterior contact faces on the shims were generally different in appearance compared to the noncontact surfaces. The contact faces had variable colors with shades of gray, black, and gold areas observed. Outboard of the contact areas, radially oriented streaks of medium gray lubricant deposits were observed, and relatively uniform medium gray deposits of lubricant were present inboard of the contact areas.

c. Fan Blade Platforms

Many of the fan blade platforms showed cracks, deformation, and fractures at the sides contacting the blade airfoils. The blade 12 fan blade platform (the platform trailing blade 13) was fractured and mostly missing. Fracture surfaces of the fan blade platforms were matte gray and rough consistent with overstress fracture.

d. Fan Blade Spacers

The fan blade spacers were present for each blade and were intact. The elastomer strips for each spacer were intact with no damage. Areas mating to the blade shims also had elastomer on the surface. Some fretting contact damage was observed on the forward face of the spacers. However, no cracks, dents, nicks, or wear, beyond limits listed in the Aircraft Maintenance Manual (Task 72-21-02-200-801-F00) were noted.

5. Scanning Electron Microscopy

a. Blade 13

After the initial optical examination described above, the fracture surface was inserted into the scanning electron microscope (SEM) for examination. An SEM image

of the origin area is shown in figure 13. The crack arrest lines that were visible by optical microscopy were also generally visible in the SEM.

At higher magnifications, striations consistent with low-cycle fatigue crack growth were observed. Typical views of fracture features within the fatigue region at various distances from the convex surface of the blade are shown in figures 14 through 16. In general, striation spacing became larger as the depth of the crack increased. However, at the crack arrest lines shown in figure 10, the striation spacing showed an abrupt change where the distance between striations immediately past each arrest line was noticeably shorter than the spacing leading up to the arrest line, consistent with a temporary reduction in crack growth rate as the crack grew after each arrest line had been formed.

Isolated areas of quasi-cleavage fracture were interspersed within the areas of striations at crack depths greater than approximately 0.14 inch. At greater crack depths, the fracture features gradually transitioned to more quasicleavage fracture with isolated areas of striations. Ductile dimples were observed in the areas of slant fracture beyond the flat fracture region bounded by arrows in figure 9.

A survey of the fracture surface was conducted along the path represented by the dashed line in figure 10 to estimate the number of striations in the region of stable fatigue crack growth. Images from the survey were then analyzed during the group phase of the examination to determine striation density at various distances from the fatigue origin.

Striation density as a function of distance from the origin for the blade 13 fracture is shown plotted in figure 17, and a power-law curve represented by a solid line was fitted to the data. By integrating the area under the curve, a total number of striations could be estimated. The locations of the crack arrest lines are also noted in figure 17 as numbered 1 through 6. For crack growth from 0.0005 inch to crack arrest line 6 at 0.263 inch, the estimated number of striations was approximately 18,400. Since one striation is usually associated with one engine flight cycle, the total number of engine flight cycles associated with crack growth is approximately equal to the estimated number of striations. Beyond, crack arrest line 4, an accurate estimate of the number of striations was not possible due to the extent of ductile tearing intermixed with the striations.

Crack arrest lines generally represent a change in stress state, environment, or time interval associated with fatigue crack growth. The blade manufacturer has reported that lubrication of the fan blade roots effectively reduces the overall stresses on the blade root in the contact areas. The number of cycles between each consecutive set of crack arrest lines on the blade 13 fracture surface was estimated by integrating the area under the curve in figure 17 along the interval defined by arrest line depths. The estimated number of cycles between arrest lines were 2,515 cycles, 1,608 cycles, 2,415 cycles, 1,769 cycles, and 2,539 cycles from arrest lines 1 to 2, 2 to 3, 3 to 4, 4 to 5, and 5 to 6, respectively. As noted in the engine history above, the intervals between the last 6 lubrication applications ranged from 1,255 cycles to 2,201 cycles, excluding the one lubrication that occurred after 98 cycles, values comparable to the estimated cycles accumulated between crack arrest lines.

Assuming that crack arrest line 6 was associated with the last blade lubrication, it was estimated that crack growth beyond crack arrest line 6 on blade 13 represented the 1,709 engine flight cycles accumulated since the last relubrication. Combining this number with the estimated 18,400 cycles associated with crack growth from 0.0005 inch to crack arrest line 6, the total number of cycles associated with crack growth from 0.0005 inch deep to failure was estimated to be approximately 20,000 cycles.

Maintenance records showed the blades had been overhauled 10,712 cycles before the accident. Given the estimated time for crack growth, it was likely a crack was present at the time of last overhaul. The estimated total cycles of crack growth from crack arrest line 2 to failure was approximately 10,000 cycles, which was within 10 percent of the cycles since overhaul. The size of the crack represented by crack arrest line 2 was 0.239 inch long axially at the blade surface with a depth of 0.068 inch.

The dovetail piece from blade 13 was repositioned in the SEM to examine the blade surface adjacent to the origin area. The surface had an irregular rough texture consistent with a grit-blast surface. When viewed using the backscattered electron detector in composition mode,[8] lighter areas consistent with deposits of Cu-Ni-In and darker areas consistent with lubricant or grit remnants were present scattered on the surface (see figure 18). In the area shown in figure 18, secondary crack features were observed as indicated with arrows.

b. Blade 20

Each of the intact blades had been inspected using UT inspection before they were transported to the NTSB Materials Laboratory. None of the blades had a UT signal response that exceeded the crack indication threshold. Among the blades tested, blade 20 had one of the highest signal responses at approximately ½ the threshold level. Therefore, blade 20 was selected for SEM examination of the blade surface for any evidence of crack features.

The forward portion of the blade root including the dovetail was sectioned from the remainder of the blade to facilitate the SEM examination. First, the coating was stripped from the dovetail to expose the underlying surface by soaking in concentrated nitric acid. Next, the surface on the convex side of the blade was etched using a solution of 15% concentrated nitric acid and 15% concentrated hydrofluoric acid added to water (15/15 reagent). Isolated microcrack features,[9] generally <100 microns long, were observed at locations ranging from 0.47 inch to 1.11 inches aft of the leading edge and 0.61 inch outboard of the root end face. Typical microcrack features are shown in the SEM image in figure 19.

[8] SEM images produced using a backscattered electron detector in composition mode have contrast that is associated with atomic weight of the elements in the image. Areas with elements having higher atomic weights appear as a relatively lighter shade of gray compared to areas having elements with lower atomic weights.
[9] A microcrack is a crack feature of microscopic proportions usually visible at magnifications of at least 50 times.

6. Metallography

a. Blade 13

Transverse cross-sections were cut through the dovetail piece of blade 13 to facilitate a metallographic examination. Metallographic samples were cut from the overstress regions at the middle of the blade and near the aft end of the contact face. The sectioned dovetail piece is shown in figure 20, and the cut faces prepared for metallographic examination are indicated. The cross-section was mounted in a polymer compound and polished followed by etching with Kroll's reagent to reveal the blade microstructure.

A macrograph of the polished and etched cross-section from the middle of the blade is shown in figure 21. The contact faces at the convex and concave sides of the dovetail are indicated with brackets.[10] As shown in figure 22, the etched microstructure for the blade 13 dovetail showed a nearly even mix of alpha grains (appearing white or light gray) interspersed with areas of alpha plus beta (brownish gray areas), consistent with the expected microstructure for the specified material after etching with Kroll's reagent. No surface anomalies, such as distorted grains or alpha case, were observed on the surfaces. Similar features were also observed in the polished and etched sample sectioned from near the aft end of the contact face.

The metallographic samples from the blade 13 dovetail were repolished to obtain a better polish condition on the Cu-Ni-In coating, and the coating was examined in the as-polished condition. The Cu-Ni-In surface coating was intact and present on the contact faces at both the convex and concave sides of the dovetail. A typical view of the coating is shown in figure 23 showing the coating near the middle of the convex contact face on the middle metallographic sample. Relatively large grit-blast particles such as the particle shown in figure 24 were observed at the interface between the coating and the substrate in a few areas. The grit-blast media used on the dovetail surface before coating during the last blade repair was 70-grit aluminum oxide.

Thickness of the Cu-Ni-In coating was measured on the cross-sections. At the middle of the blade, the thickness measured 0.0053 inch to 0.0061 inch on the convex side and 0.0046 inch to 0.0049 inch on the concave side. On the cross-section from the aft end of the contact face, the thickness measured 0.0035 inch to 0.0056 inch on the convex side and 0.0044 inch to 0.0049 inch on the concave side. According to coating specifications, the thickness of the coating after application should be between 0.0047 inch and 0.0071 inch (0.12 millimeters and 0.18 millimeters).

[10] Due to the imaging characteristics of the inverted metallograph used to create the macrograph in figure 21, the macrograph is a mirror image to that observed by direct observation of the mounted sample on the plane indicated in figure 20.

b. Blade 20

The root end of blade 20 that had been examined using the SEM was sectioned to prepare a metallographic examination of the cross-section approximately 0.5 inch aft of the leading edge. A view of the blade 20 piece after sectioning is shown in figure 25. The specimen was mounted in a polymer material and was polished to facilitate an examination of the cross-section at the convex surface for evidence of microcracks. No crack features were observed after the first polish, but the sample was repolished from the grinding step (120 grit) and reexamined. In the repolished sample, one microcrack was observed as shown in figure 26. The microcrack had a depth of 0.001 inch in the plane of the polish and was located 0.61 inch from the root end face.

7. Nondestructive Inspections

Nondestructive inspections (NDI) were conducted on the roots of the remaining intact blades (not including blade 20, which was sectioned for SEM and metallographic examinations as described in the previous subsections) using FPI, UT, and ECI to inspect for cracks in the blade root on both the concave and convex sides. Procedures used for the inspections were consistent with UT inspections conducted during blade lubrication and with FPI and ECI procedures conducted during blade overhaul. No confirmed cracks were detected as a result of these inspections as described below.

The remaining intact blades were shipped to the GE Engineering Materials Systems laboratory where the Cu-Ni-In coatings on the dovetails were stripped by soaking in concentrated nitric acid. Many of the blade dovetails had visual damage consistent with sliding contact and impact damage on the contact faces corresponding to blade dovetail movements within the fan disk slots.

The blade roots were then inspected by ECI at the GE laboratory. Blades 1, 2, 3, 5, 10, 11, 12, 15, 21, 22, 23, and 24 had an ECI signal response that was above the threshold for rejection. However in most cases, the signal response above threshold was associated with a visual surface anomaly such as sliding contact or impact damage. No surface anomaly was associated with an above-threshold response on blades 2, 10, and 11. These above-threshold responses in blades 2, 10, and 11 were located on the concave side 3.5 inches from the leading edge, on the concave side 2.7 inches from the leading edge, and on the convex side 0.25 inch from the leading edge near an undercut, respectively.

Next, the remaining intact blades were shipped to the Safran Aircraft Engines Failure Analysis Laboratory for photography, UT, FPI, and additional ECI. On the dovetails with stripped coating, disturbance of the underlying material was noted particularly near the leading and trailing edges of blades 18 through 24 and 1 through 4.

Above-threshold signal responses were detected with ECI on blades 1, 2, 3, 5, 12, 15, 16, 21, 22, 23, and 24. In most cases, the above-threshold response was associated with a visual disturbance or impact. No indications consistent with a preexisting crack were detected by ECI. FPI indications were detected in blades 1, 2, 3, and 23, and each

of the indications appeared to be associated with impacts or surface disturbances. UT signal responses detected on blades 1, 5, 12, 21, and 23 were ½ or less of the crack indication threshold. Blades with ECI or FPI indications were further examined by etching the surface with 15/15 reagent followed by an optical examination of the surface using a stereo microscope. No evidence of cracks or microcracks were observed in the areas with NDI indications.

8. Metallography of Blades 3, 12, 23, and 24

Based on the NDI results and blade characteristics, blades 3, 12, 23, and 24 were selected for metallographic examination. Features consistent with material overlap or smearing were observed in areas associated with surface disturbances in the cross-sections. No evidence of fatigue microcracks were observed.

9. Residual Stress Measurements

Residual stress measurements obtained by X-ray diffraction at the surface and at varying depths up to approximately 0.0083 inch (211 micrometers) were conducted at Lambda Technologies in Cincinnati, Ohio, and at the Safran Materials and Processes Laboratory in Evry Corbeil and Vernon, France. Residual stress measurements, measured in the radial and/or longitudinal direction, were completed on blades 13 and 20 at Lambda Technologies, and on blades 3, 12, 23, and 24 at Safran. The measurements were compared to reference residual stress depth profile data, supplied by Safran, for blades that were peened in accordance with specified parameters.

Residual stress measurements were taken on multiple areas of the dovetail surfaces. On blades 13 and 20, the measurements were taken near the middle of the contact face on the convex side approximately 0.5 inch and 2 inches from the leading edge. On blades 3, 12, 23, and 24, measurements were taken near the outboard side of the contact face at two locations on the convex side and 1 location on the concave side. On the convex side, the measurement locations were approximately 0.5 inch and 2 inches away from the leading edge. On the concave side, the measurement location was approximately 1 inch forward of the blade axial retention slot. The Cu-Ni-In coating on blade 13 was stripped by soaking in concentrated nitric acid before testing for residual stress. The coatings on the remaining blades had been previously stripped for optical examination and NDI.

Results of the residual stress measurements are shown plotted in figure 27. Abnormal residual stress profiles including residual tension near the surface were observed in one or more locations on each of the intact blades tested from the accident engine when compared to the reference profile. Minimum residual stress values (most compressive) from the residual stress profile measurements are listed in table 4. In many cases, the minimum residual stress value was higher (less compressive) than the expected minimum value, which is expected to be no greater than -500 megapascals. In table 4, the residual stress profiles with a minimum residual stress value that was above -500 megapascals (abnormal profile) are highlighted in yellow, and the profiles with a minimum residual stress value below -500 megapascals (expected profile) are

highlighted in green. The additional loads on a fan blade resulting from a blade out event can affect residual stress profiles. The residual stress profile for fractured blade 13 was comparable to the reference residual stress profile. However, all 24 blades in the set had been shot-peened during the last overhaul, and the overhaul occurred after the crack initiated based on service history data and crack growth estimates derived from the fractographic examination.

Table 1. Residual Stress Measurement Results

Blade	Side	Distance from LE (inch)	Distance from TE slot (inch)	Test Lab	Residual Stress at a 10-micrometer Depth (MPa)	Minimum Residual Stress Value (MPa)
3	CVX	0.5		Safran	-260	-350
3	CVX	2		Safran	-396	-550
3	CCV		1	Safran	47 (tension)	40 (tension)
12	CVX	0.5		Safran	127 (tension)	120 (tension)
12	CVX	2		Safran	63 (tension)	30 (tension)
12	CCV		1	Safran	-327	-480
13	CVX	0.5		Lambda	-608	-647
13	CVX	2		Lambda	-499	-562
20	CVX	0.5		Lambda	-361	-432
20	CVX	2		Lambda	-480	-539
23	CVX	0.5		Safran	178 (tension)	140 (tension)
23	CVX	2		Safran	-453	-500
23	CCV		1	Safran	33 (tension)	10 (tension)
24	CVX	0.5		Safran	210 (tension)	180 (tension)
24	CVX	2		Safran	-305	-410
24	CCV		1	Safran	-183	-240
Ref.				Safran	-596	-675

10. Field Inspection Findings

Blades with confirmed cracks from fan blade field inspections reported on or after April 20, 2018 will be documented in this section. Previous field inspection findings reported before April 20, 2018 were documented in Materials Laboratory Factual Report 17-043 associated with an accident (DCA16FA217) that occurred on August 27, 2016 involving a fan blade fracture on another Boeing 737-700 airplane powered by CFM International CFM56-7B engines. The August 27, 2016 accident flight was operated as Southwest Airlines flight number 3472 and was diverted to Pensacola International Airport, Pensacola, Florida after the engine failure.

In November 2016 after a tool for routine and repeatable ECI of the blade root was developed and available to the overhaul shops, ECI was added to the overhaul process. In March 2017, a service bulletin was issued to require UT at each blade lubrication for

all fan blades with at least 9,000 engine flight cycles since the last shop visit. The service bulletin was revised in June 2017 to limit the UT inspections to fan blades with at least 15,000 engine flight cycles since last shop visit. On April 20, 2018, a service bulletin was issued to require UT inspections at blade lubrication for all blades with at least 20,000 cycles.

Since the accident on April 20, 2018, 2 blades with confirmed cracks have been found through ECI at overhaul and an additional 2 blades with confirmed cracks have been detected by UT during blade lubrication. The cracks were all located in the shot-peened and grit blast area of the dovetail 0.552 inch to 0.598 from the root end face. For reference in this report, the blades will be labeled M through P[11] in chronological order by the date the crack indication was reported.

On April 22, 2018, blade M, owned by a domestic operator (not Southwest Airlines), was removed from service after a crack indication was detected during UT inspection at blade lubrication. Blade M had originally been manufactured as a part number 340-001-022 fan blade and had rework resulting in a part number change to 340-001-039. The blade had accumulated approximately 57,998 hours TSN and 22,072 CSN. The blade had been repaired at GKN in August 2007 and again in December 2014. The blade had accumulated 3,889 cycles since the last repair and had accumulated 11,748 cycles since the repair in 2007.

The UT indication was located on the convex side of the blade approximately 2.2 inches from the forward end. The blade was sent to the GE Engineering Materials Systems laboratory for examination. Prior to receipt at the GE laboratory, the Cu-Ni-In coating was stripped to facilitate additional NDI, and crack indications were detected using FPI and ECI. Next, the area of the UT indication was sectioned from the rest of the dovetail and the surface was etched using a modified Kroll's reagent for SEM examination. A crack approximately 0.386 inch long in the area of the UT indication was observed. The crack was surrounded by a network of microcracks. The crack and most of the microcracks were all located in the peened and grit blast region near the outboard edge of the contact face previously covered by the Cu-Ni-In coating, however some microcracks were also detected just outboard of the grit blast region in an area that was shot-peened only. The location of the microcracks in the current shot-peened only were within the range of allowable shot-peened and grit blast area and may have formed within a previous grit blast region at some time before the last repair in 2014.

Next, the dovetail in the area of cracking was sectioned to facilitate a lab fracture to open the crack. Views of the resulting fracture surface are shown in figure 28. A portion of the fracture surface had a flat fracture with curving boundaries, features consistent with fatigue. The crack emanated from multiple origins located at the blade surface as indicated with an unlabeled brackets in figure 28. The lab cut used to open the crack intersected the crack tip at the location of deepest penetration. As shown in figure 28, the crack extended approximately 0.116 inch deep and was 0.386 inch long at the surface. Two prominent crack arrest lines were visible on the surface, indicated with

[11] Letters A through L were used to reference fan blades in Materials Laboratory Factual Report 17-043.

unlabeled arrows in figure 28. The first and second crack arrest lines extended up to approximately 0.040 inch deep and 0.073 inch deep, respectively.

The fracture surface was examined using an SEM, and features consistent with low-cycle fatigue were observed. The fracture features in the fatigue region were surveyed to estimate the number of striations within the region of crack growth. Striation density as a function of distance from the origin for the blade M crack is shown plotted in figure 29, and a logarithmic curve was fitted to the data as indicated by the orange dashed line. By integrating the equation for the curve fitted to the blade M data from a depth of 0.0005 inch to the crack tip at 0.116 inch, the total number of cycles of crack growth was estimated to be approximately 9,000 cycles. Locations of the crack arrest lines are also indicated on the plot.

A transverse cross-section was cut through the dovetail of blade M near the forward end of the crack. The polished and etched cross-section showed a typical microstructure for the specified Ti-6-4 alloy with no surface anomalies. Several microcracks were observed emanating from the surface with measured depths up to 0.0014 inch deep.

Next, the blade M dovetail was sent to the Safran Aircraft Engines laboratory for residual stress analysis. Residual stress in the radial and longitudinal directions were obtained on the convex side of the dovetail in the contact face at 2 locations forward of the segment that had been removed for the fractographic and metallographic examinations and at 1 location near the aft end of the contact face. Measurements in both all 2 locations in both the radial and longitudinal directions showed residual stress profiles that had a shape comparable to the reference residual stress profile (see figure 27) with minimum residual stress values of approximately -600 megapascals. Although a profile comparable to the reference profile was obtained, the blade had been shot-peened during the last overhaul, and the overhaul occurred after the crack initiated based on service history data and crack growth estimates derived from the fractographic examination.

Around the time of the blade M discovery, blade N, owned by a foreign operator, was reported to have an ECI indication found during blade overhaul. Blade N had originally been manufactured as a part number 340-001-022 fan blade and had rework resulting in a part number change to 340-001-037. The blade had accumulated approximately 31,697 CSN. The blade had been overhauled at GKN in June 2006 and at Safran in November 2013. The blade had accumulated 9,216 cycles since the last overhaul.

Blade N was sent to Safran Aircraft Engines laboratory for examination. The crack indication was located approximately 2.4 inches aft of the forward face and was approximately 0.20 inches long. After etching with 15/15 reagent, a network of cracks was visible under optical magnification. The cracks were located in the shot peened and grit blasted surface.

The dovetail of blade N was sectioned to facilitate a lab fracture to expose the crack fracture features, and the resulting fracture surface is shown in figure 30. The crack had multiple origins located at the blade surface as indicated with unlabeled brackets in figure 30 and extended to a maximum depth of 0.033 inch and an axial length of 0.224 inch at the blade surface.

The crack fracture surface was examined using an SEM, and features consistent with low-cycle fatigue were observed. However, fracture features near the origin were damaged by post-fracture surface recontact and were obscured by coating deposits on the surface. The fracture features in the fatigue region were surveyed to estimate the number of striations within the region of crack growth. Striation density as a function of distance from the origin for the blade N crack is shown plotted in figure 31, and an exponential curve was fitted to the data as indicated by the solid line. By integrating the equation for the curve fitted to the blade N data from a depth of 0.0005 inch to the crack tip at 0.033 inch, the total number of cycles of crack growth was estimated to be approximately 6,700 cycles.

Residual stress measurements in the longitudinal direction were obtained on the convex side of the dovetail in the contact face near the leading edge and at two locations near the area of cracking. A measurement was also made on the concave side opposite the area of cracking. The residual stress profiles at each of the locations had a shape comparable to the reference residual stress profile (see figure 27) with minimum residual stress values ranging from -600 megapascals to -650 megapascals. Attempts to determine if the crack in blade N had initiated prior to the last blade overhaul were inconclusive.

On April 25, 2018, blade O, owned by Southwest Airlines, was removed from service after a crack indication was detected during UT inspection at relubrication. Blade O had originally been manufactured as a part number 340-001-022 blade and had rework resulting in a part number change to 340-001-039. The blade had accumulated approximately 59,722 hours TSN and 34,770 CSN. The blade had been repaired at GKN in September 2017 and had passed the required ECI inspection. The blade had also been overhauled at GKN in March 2009. The blade had accumulated 302 cycles since the last overhaul and had accumulated 16,642 cycles since the overhaul in 2009.

The UT indication was located on the convex side of the blade approximately 2.3 inches from the forward end. The blade was sent to the GE Engineering Materials Systems laboratory for examination. Prior to receipt at the GE laboratory, the Cu-Ni-In coating was stripped to facilitate additional NDI, and crack indications were detected using UT and ECI. Next, the area of the UT indication was sectioned from the rest of the dovetail and the surface for SEM examination. Initially the examination for crack features was difficult due to embedded media on the surface. After etching using a modified Kroll's reagent, a band of microcracking approximately 0.040 inch wide and 0.7 inch long was observed in the shot peened and grit-blasted surface in the area of the UT indication. A well-defined crack approximately 0.362 inch long was also observed within the band of microcracking.

Next, the dovetail in the area of the crack was sectioned to facilitate a lab fracture to open the crack. Views of the resulting fracture surface are shown in figure 32. A portion of the fracture surface had a flat fracture with curving boundaries, features consistent with fatigue. The crack emanated from multiple origins located at the blade surface as indicated with an unlabeled bracket in figure 32. A dashed line in figure 32 indicates the crack boundary, which had multiple curving fronts extending up to 0.030 inch deep and extending 0.362 inch long at the surface.

The fracture surface was examined using an SEM, and features consistent with low-cycle fatigue were observed. The fracture features in the fatigue region were surveyed to estimate the number of striations within the region of crack growth. Striation density as a function of distance from the origin for the blade O crack is shown plotted in figure 33, and a power-law curve was fitted to the data as indicated by the solid line. By integrating the power-law equation for the curve fitted to the blade O data from a depth of 0.0005 inch to the crack tip at 0.030 inch, the total number of cycles of crack growth was estimated to be approximately 7,800 cycles.

A transverse cross-section was cut through the dovetail of blade O near the forward end of the crack. The polished and etched cross-section showed a typical microstructure for the specified Ti-6-4 alloy with no surface anomalies. Particles consistent with grit blast media approximately 0.00075 inch in size were observed embedded on the surface in the grit-blast area of the dovetail.

In June 2018, blade P was reported to have an ECI indication found near the aft end of the blade on the concave side. Blade P had originally been manufactured as a part number 340-001-022 fan blade and had rework resulting in a part number change to 340-001-027. The blade had accumulated approximately 66,334 hours TSN and 38,936 CSN. The blade had been overhauled at GKN in September 2009 had accumulated 17,530 cycles since the last overhaul.

Blade P was sent to Safran Aircraft Engines laboratory for examination. The crack indication was located approximately 1.6 inches forward of the axial retaining groove on the concave side of the blade as shown in figure 34 and was detected using UT, ECI, and FPI before etching. After etching with 15/15 reagent, a network of cracks in a band approximately 0.63 inch long and 0.08 inch wide was visible under optical magnification. The microcracks were located in the shot peened and grit blasted surface, and the main crack was located within the network of microcracks.

The dovetail of blade P was sectioned to facilitate a lab fracture to expose the crack fracture features, and the resulting fracture surface is shown in figure 35. The crack had multiple origins located at the blade surface and extended to a maximum depth of 0.059 inch and an axial length of 0.417 inch at the blade surface. A crack arrest line was observed as indicated with unlabeled arrows in figure 35 at a depth of up to 0.042 inch.

The crack fracture surface was examined using an SEM, and features consistent with low-cycle fatigue were observed. Fracture features near the origin were slightly damaged by post-fracture surface recontact. The fracture features in the fatigue region were surveyed to estimate the number of striations within the region of crack growth. Striation density as a function of distance from the origin for the blade P crack is shown plotted in figure 36, and a power-law curve was fitted to the data as indicated by the solid line. By integrating the power-law equation for the curve fitted to the blade P data from a depth of 0.0005 inch to the crack tip at 0.059 inch, the total number of cycles of crack growth was estimated to be approximately 15,000 cycles. Overall, the rate of crack propagation was slower than what was observed on the other blades where cracks had initiated at the convex side of the blade near the forward end.

A transverse cross-section was cut through the dovetail of blade P near the forward end of the crack. The polished and etched cross-section showed a typical microstructure for the specified Ti-6-4 alloy with no surface anomalies. Hard particles consistent with grit blast media were noted at the surface embedded up to approximately 0.001 inch maximum depth in the grit blast area of the dovetail.

Residual stress measurements were obtained on the convex side of the dovetail in the contact face near the leading edge at locations approximately 0.5 inch and 2 inches from the forward face and on the concave side contact face inboard of the area of cracking. The residual stress profiles at each location were not consistent with the reference profile with minimum values that were higher (less compressive) than the reference profile shown in figure 27. On the convex side located 0.5 inch from the forward edge, the minimum residual stress was approximately -480 megapascals. At the location 2 inches from the leading edge on the convex side and at the crack location near the aft end on the concave side, the minimum residual stress was approximately -200 megapascals. In the reference residual stress profile shown in figure 27, the minimum residual stress is -675 megapascals.

Matthew R. Fox
Senior Materials Engineer

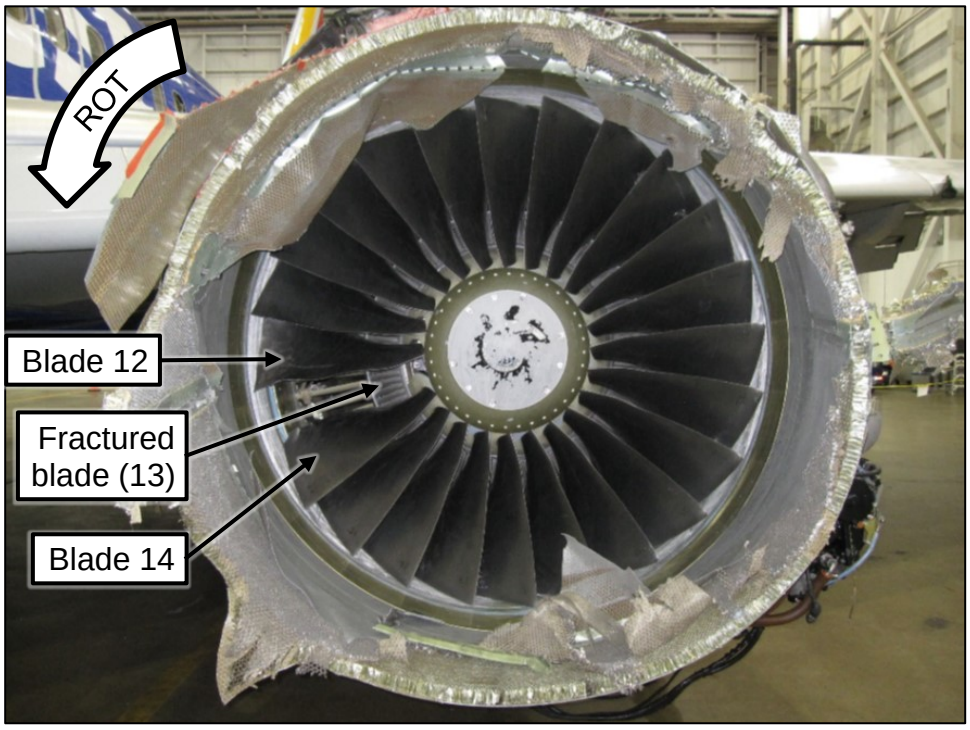

Figure 1. Overall view of the forward end of the number 1 engine after the accident.

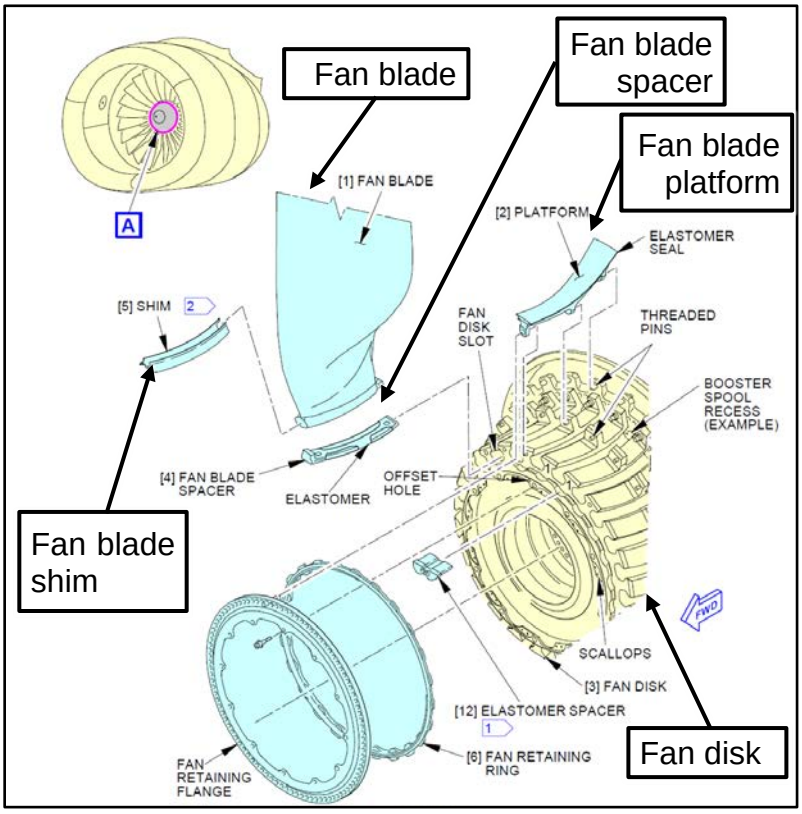

Figure 2. Fan components in the CFM56-7B engine as presented in the Boeing Aircraft Maintenance Manual.

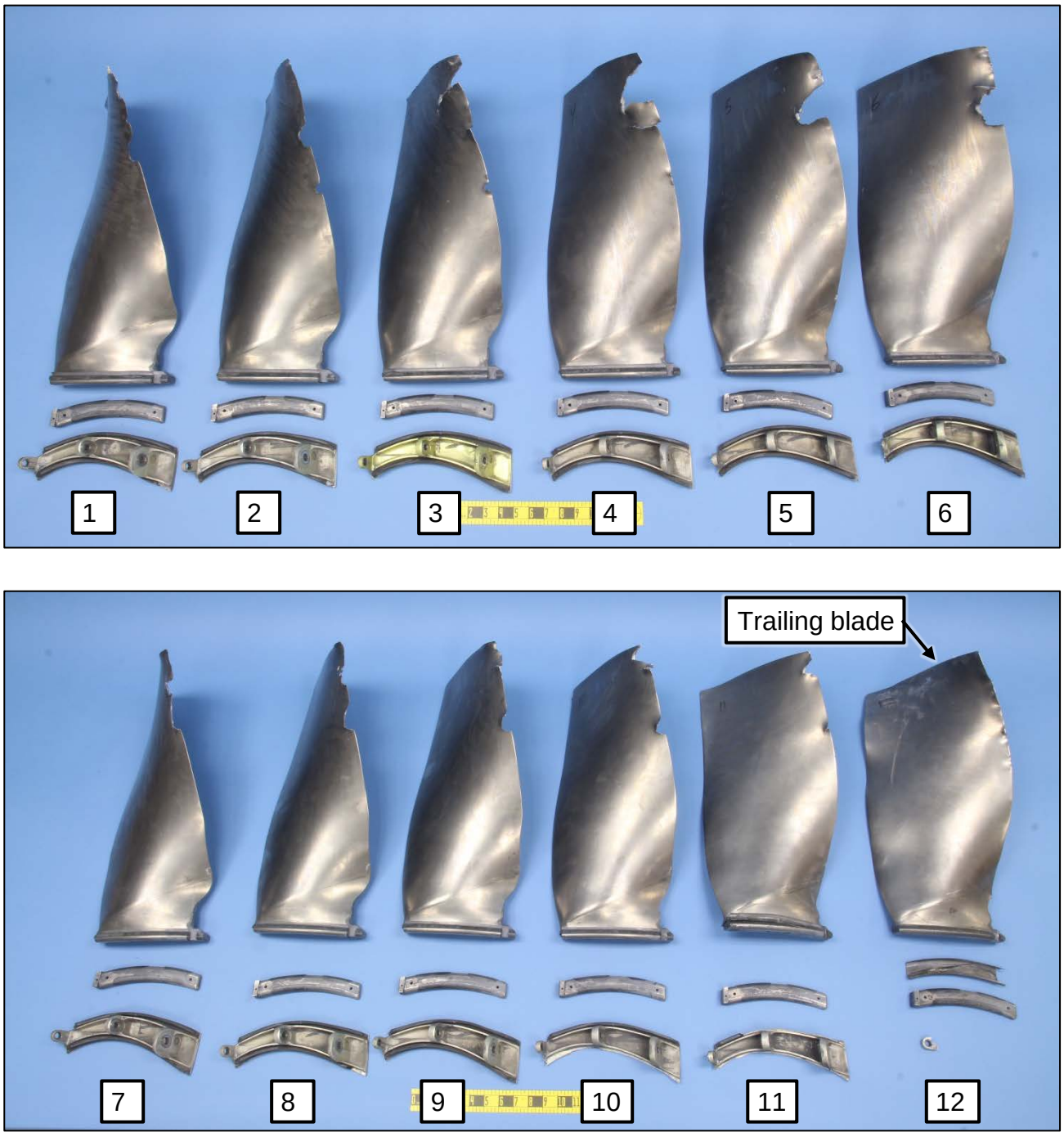

Figure 3. Overall view of submitted fan blades, fan blade spacers, fan blade shims, and fan blade platforms (shown positioned from top to bottom in each image) for blades 1 through 12. The shims are shown as-received on the dovetails. The blade trailing the fractured blade 13 is indicated.

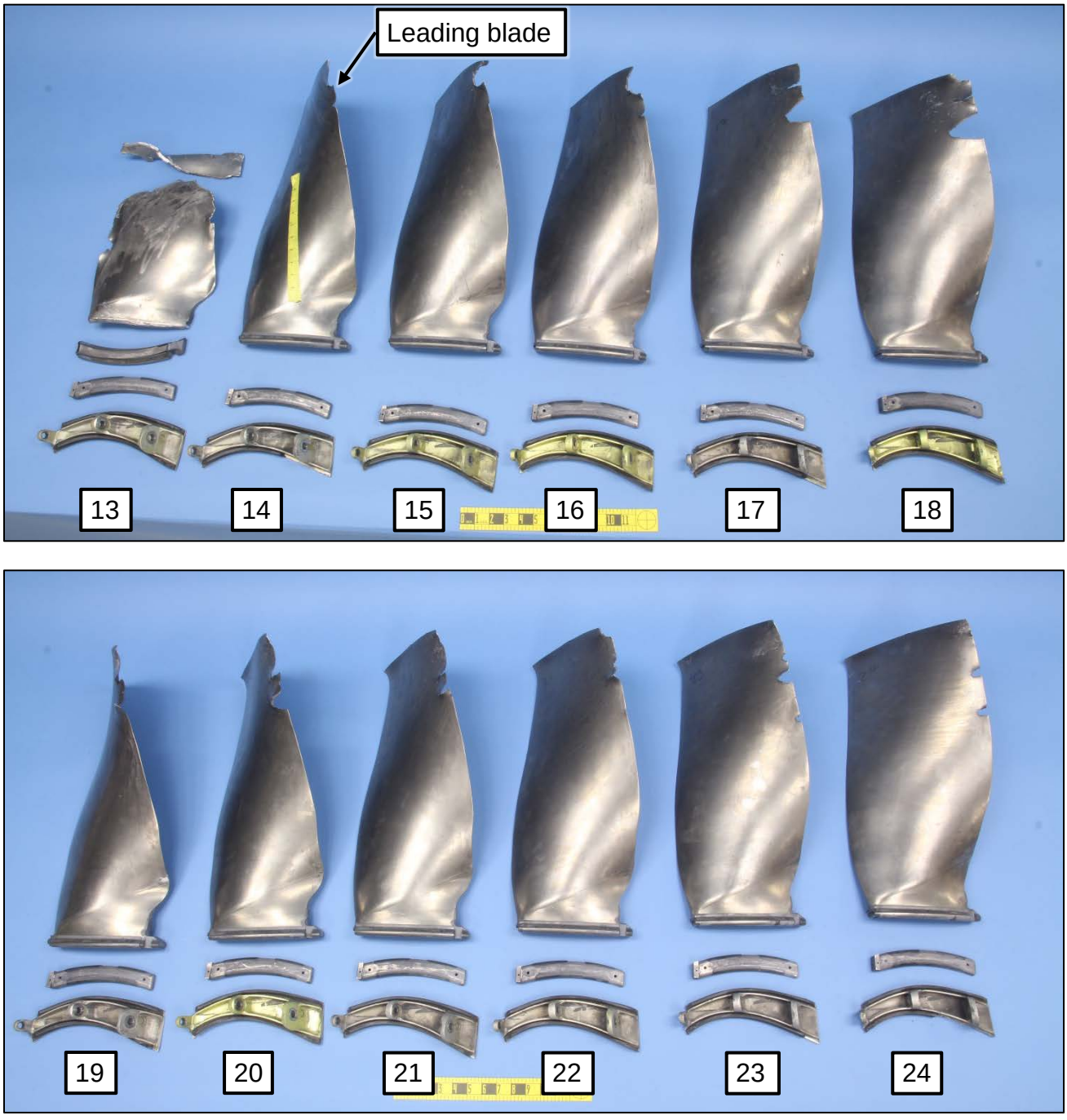

Figure 4. Overall view of submitted fan blades, fan blade spacers, fan blade shims, and fan blade platforms (shown positioned from top to bottom in each image) for blades 13 through 24. The shims are shown as-received on the dovetails. The blade leading the fractured blade 13 is indicated.

Figure 5. Closer view of the recovered blade 13 pieces and corresponding blade shim (image to the right) and markings on the root end face of the dovetail piece (lower image).

Figure 6. Overall view of the blade 13 fracture surface after cleaning. A bracket indicates the fatigue origin area located approximately 0.57 inches aft of the forward end on the convex side of the blade.

Figure 7. Overall view of the convex sides of the blade 13 dovetail piece and fan blade shim after the shim was disassembled from the dovetail.

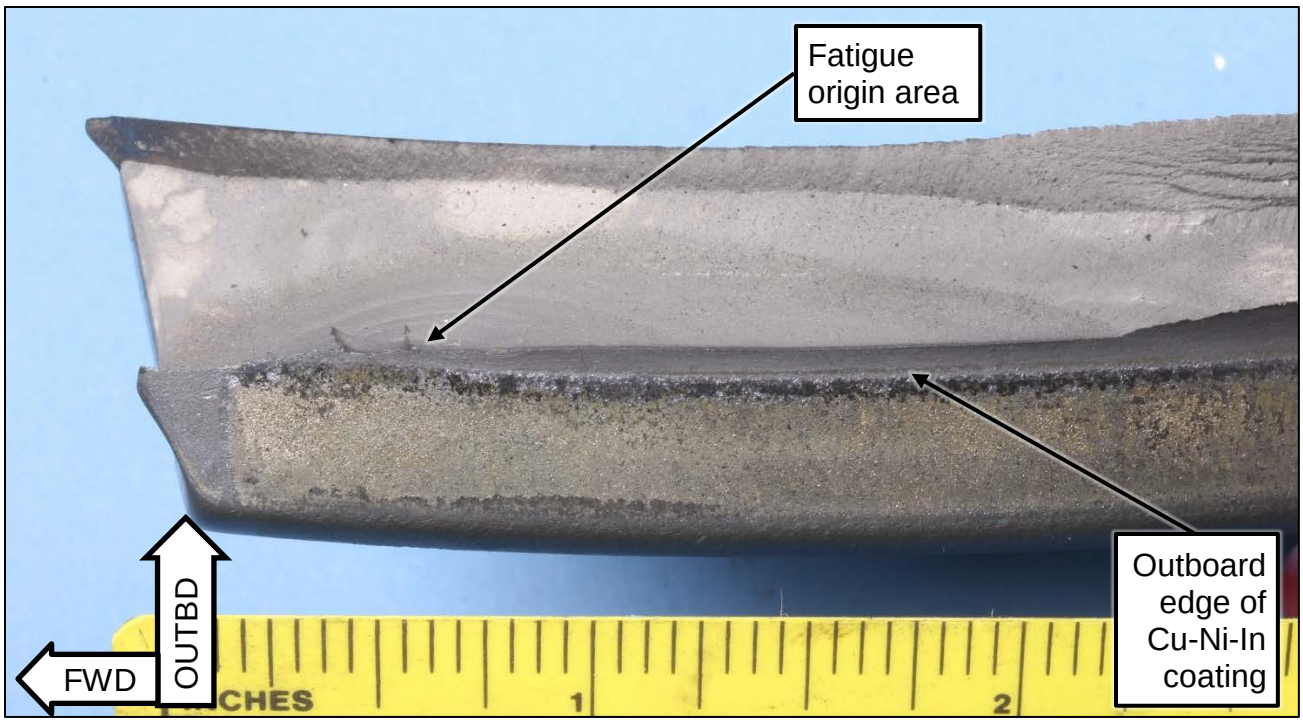

Figure 8. View of the convex face of the blade 13 dovetail at the fatigue origin area.

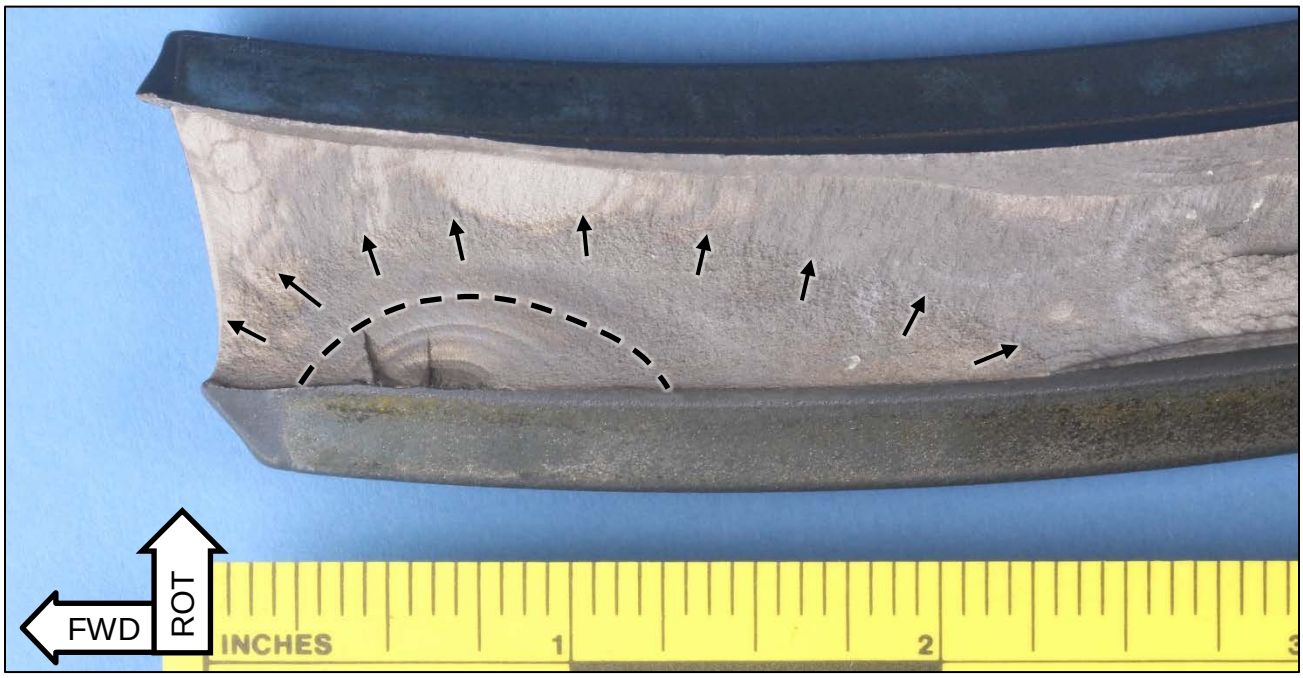

Figure 9. Close view of the fatigue region. A dashed line indicates the location of the last well-defined crack arrest mark.

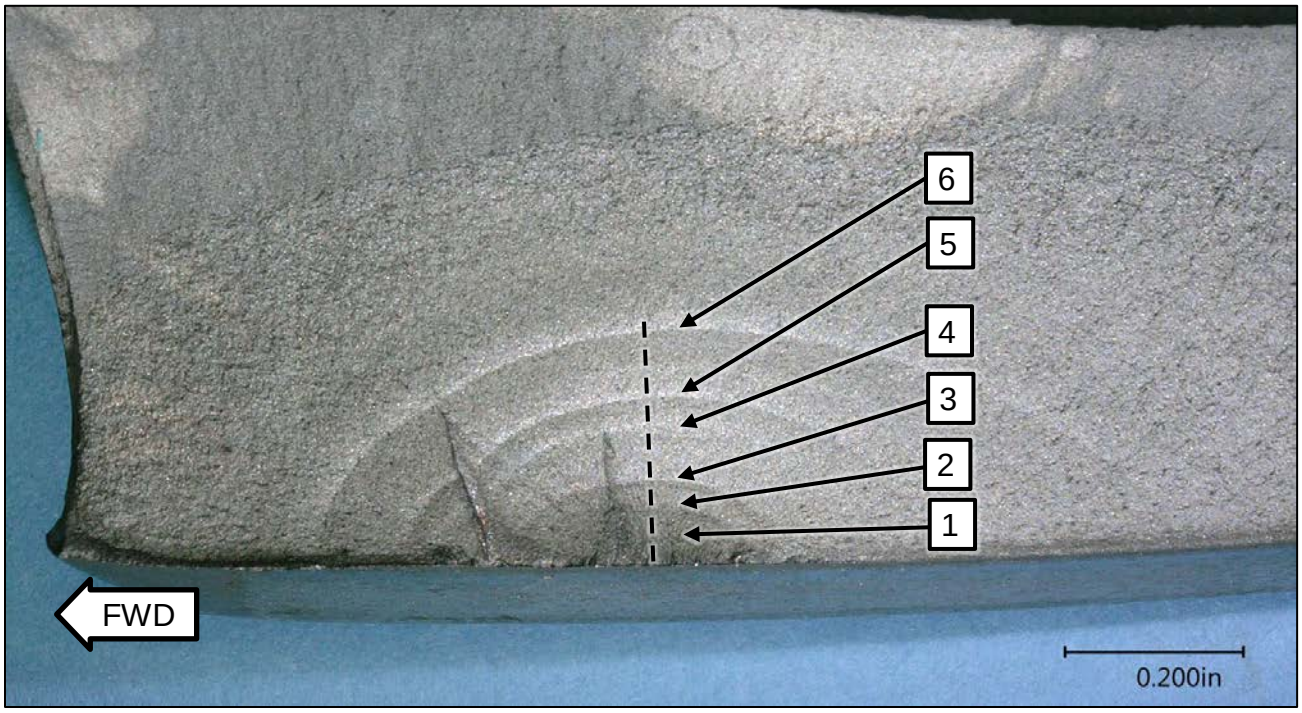

Figure 10. Close view of the cleaned origin area on blade 13. Distinct crack arrest lines are numbered, and a dashed line indicates the location where striation density was counted.

Figure 11. View of the dovetail and shim for the blade trailing the fractured blade. Pieces of the shim were fractured and missing.

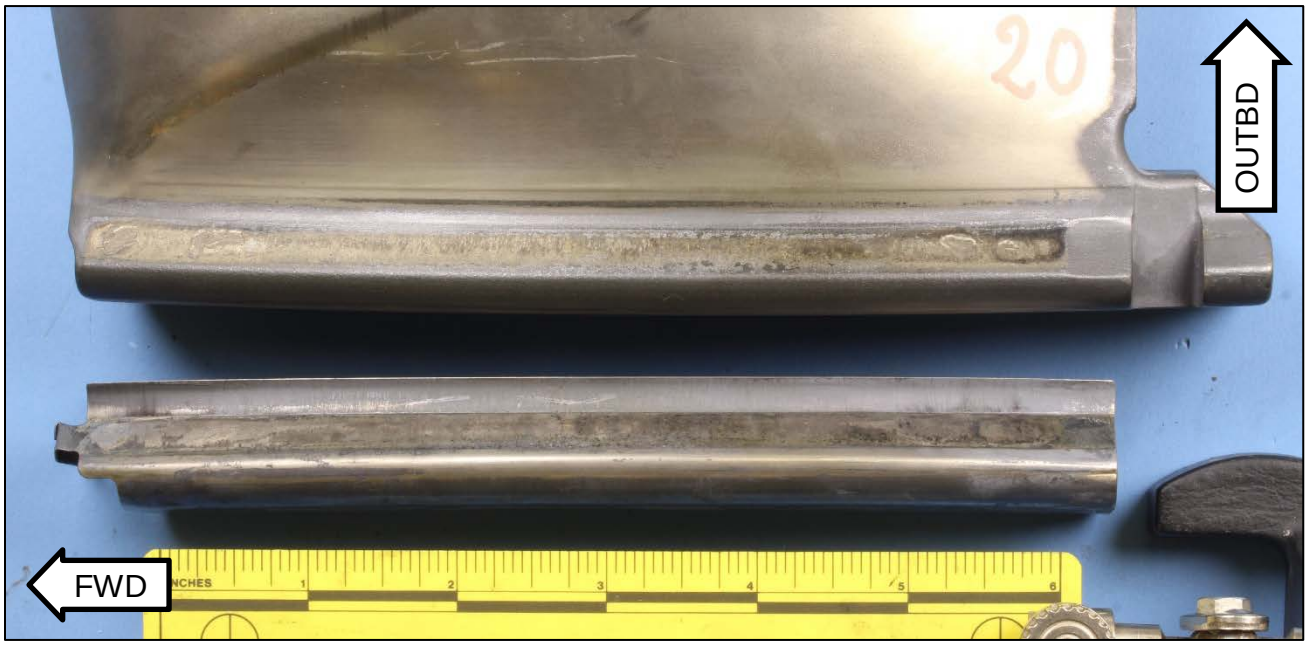

Figure 12. View of the blade 20 dovetail and shim. The Cu-Ni-In coating was disturbed near the forward and aft ends of the contact face.

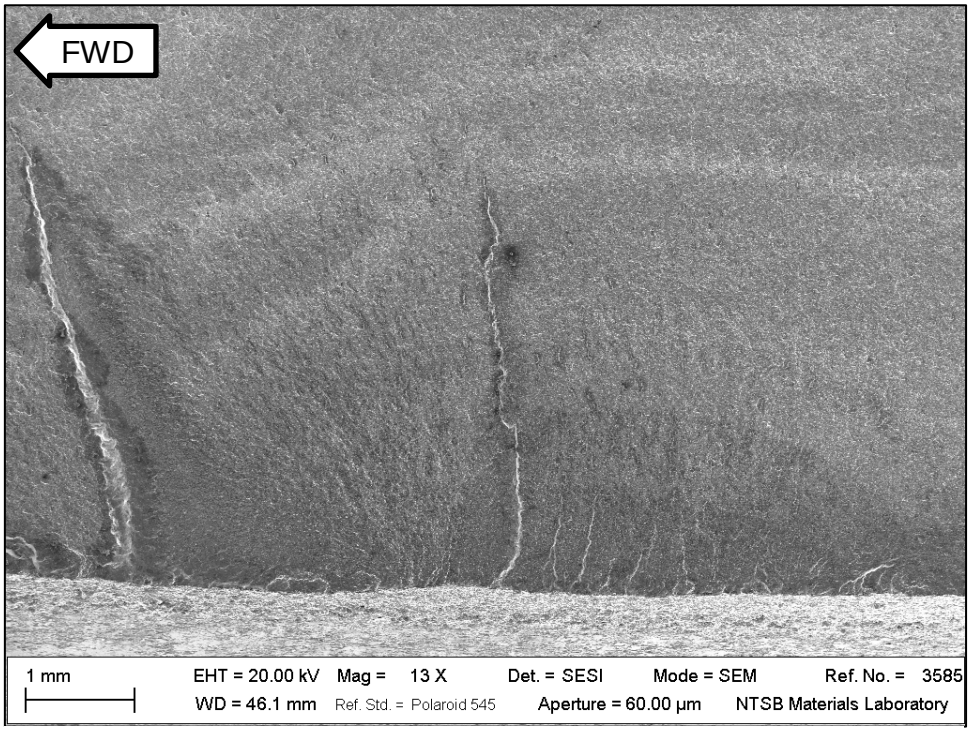

Figure 13. Overall view of the origin area after cleaning as viewed using an SEM.

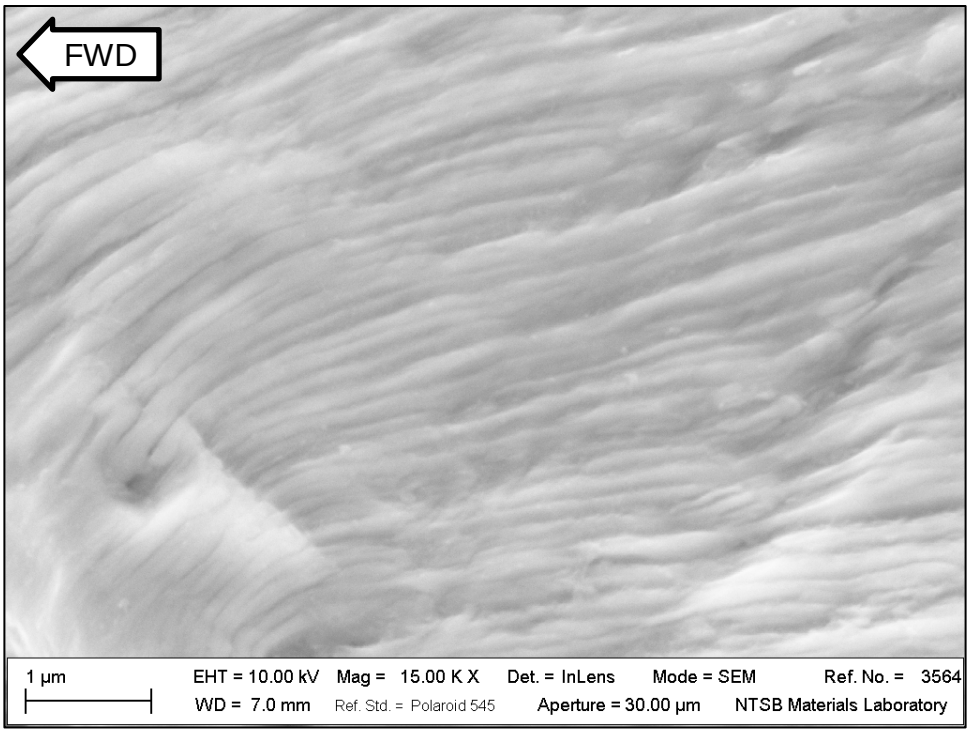

Figure 14. SEM image of the blade 13 fracture surface at 0.0124 inch from the convex surface.

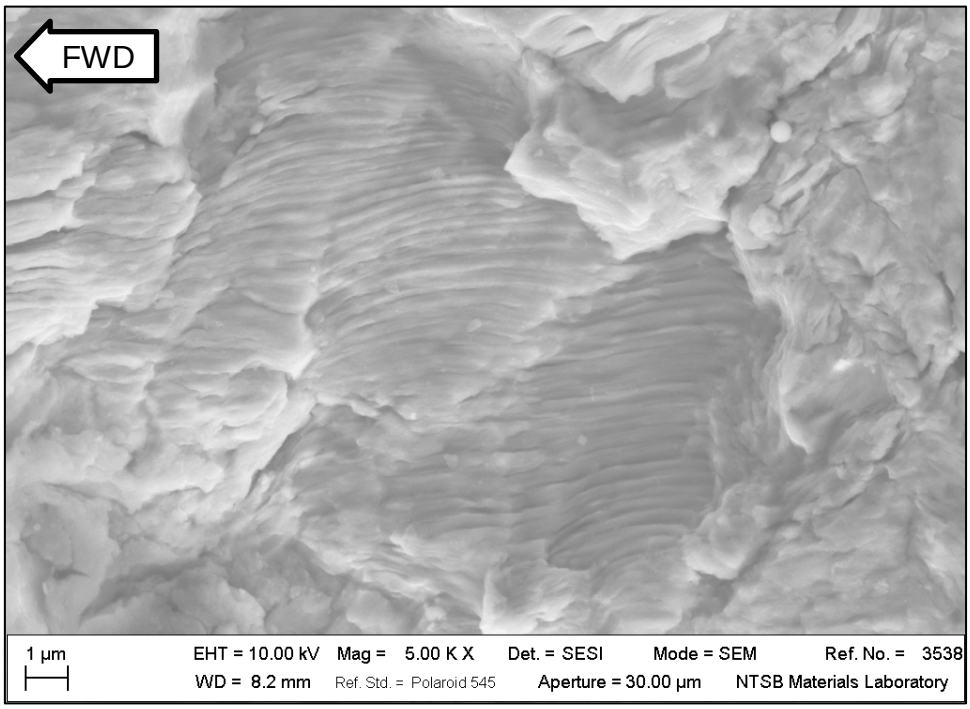

Figure 15. SEM image of the blade 13 fracture surface at 0.123 inch from the convex surface.

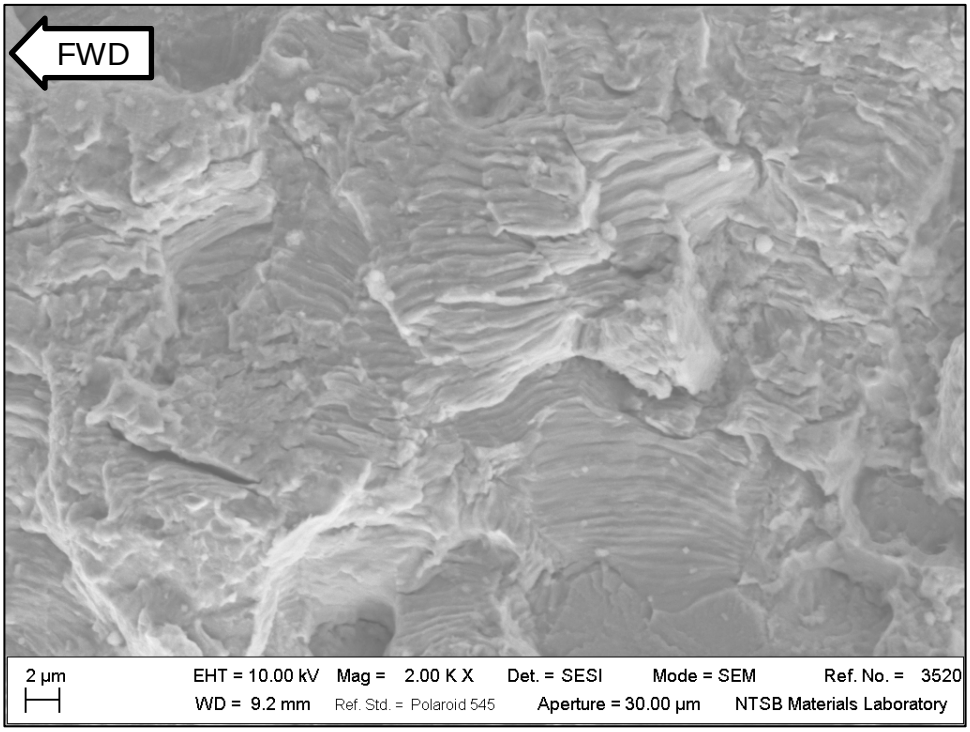

Figure 16. SEM image of the blade 13 fracture surface at 0.256 inch from the convex surface.

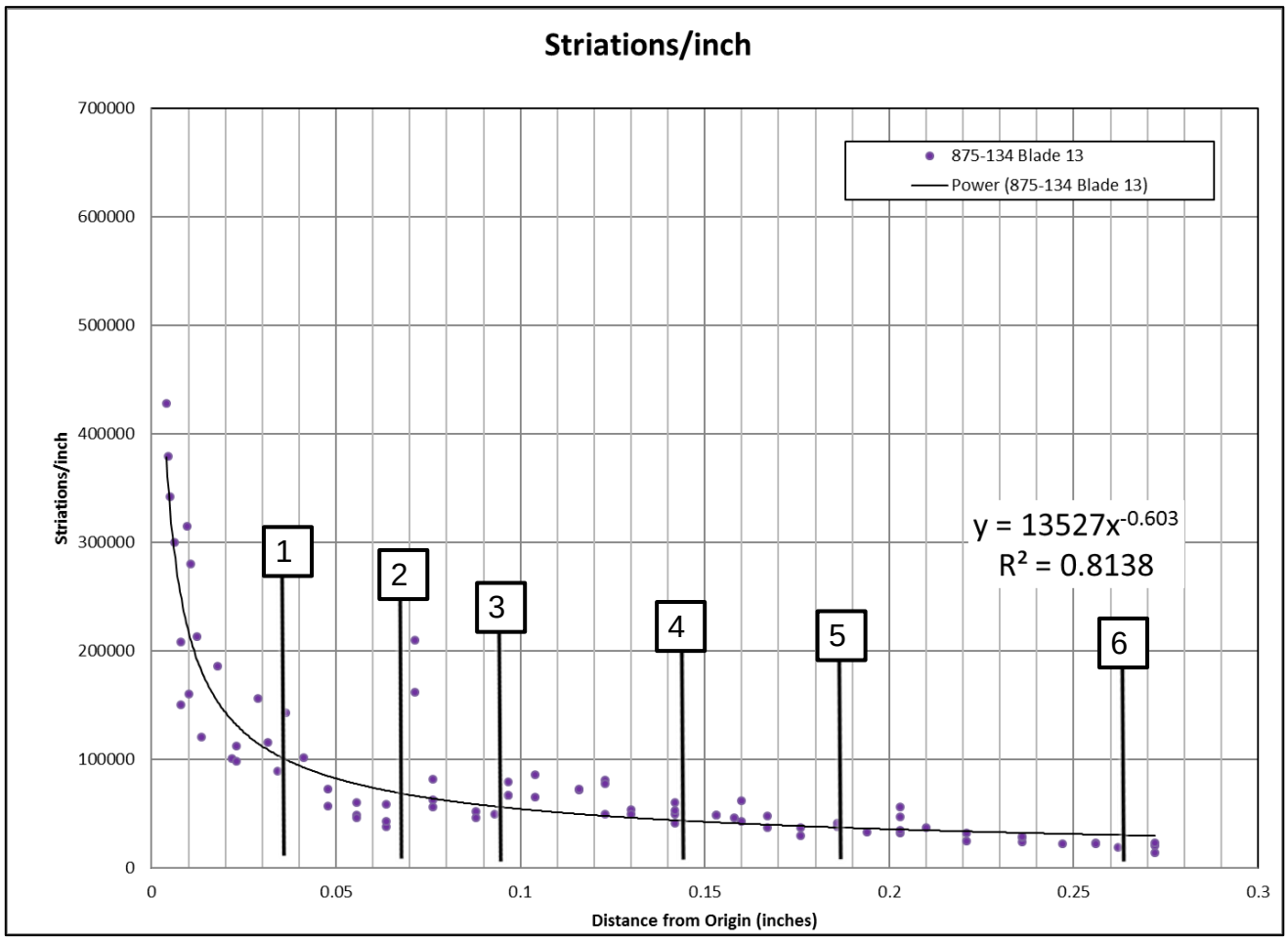

Figure 17. Striation density as a function of distance from the origin for blade 13. Locations of crack arrest lines 1 through 6 are noted on the graph.

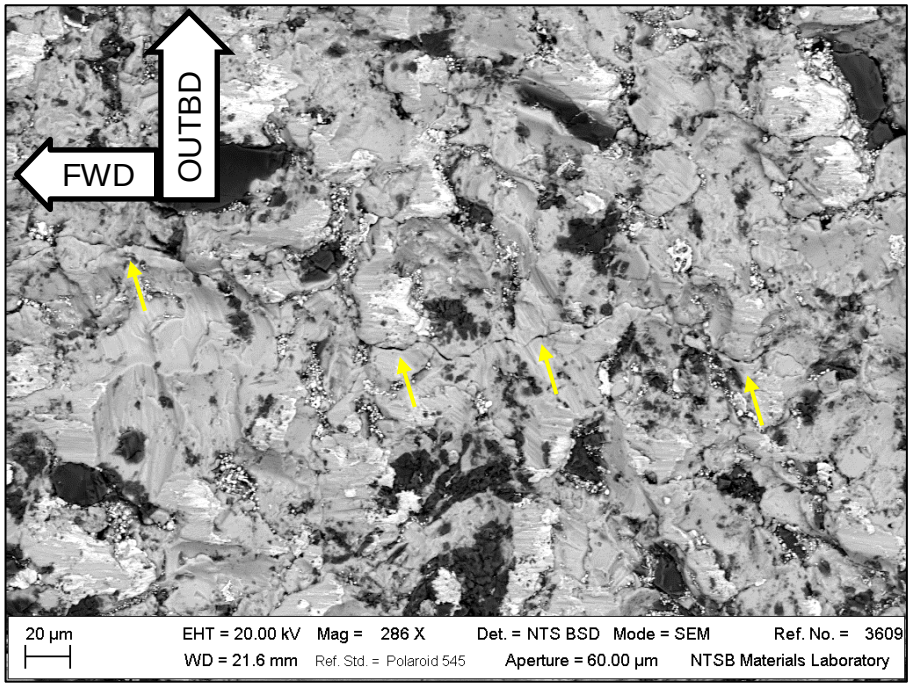

Figure 18. SEM images of a secondary crack feature observed on the surface of blade 13 adjacent to the origin area as viewed using backscattered electron detector.

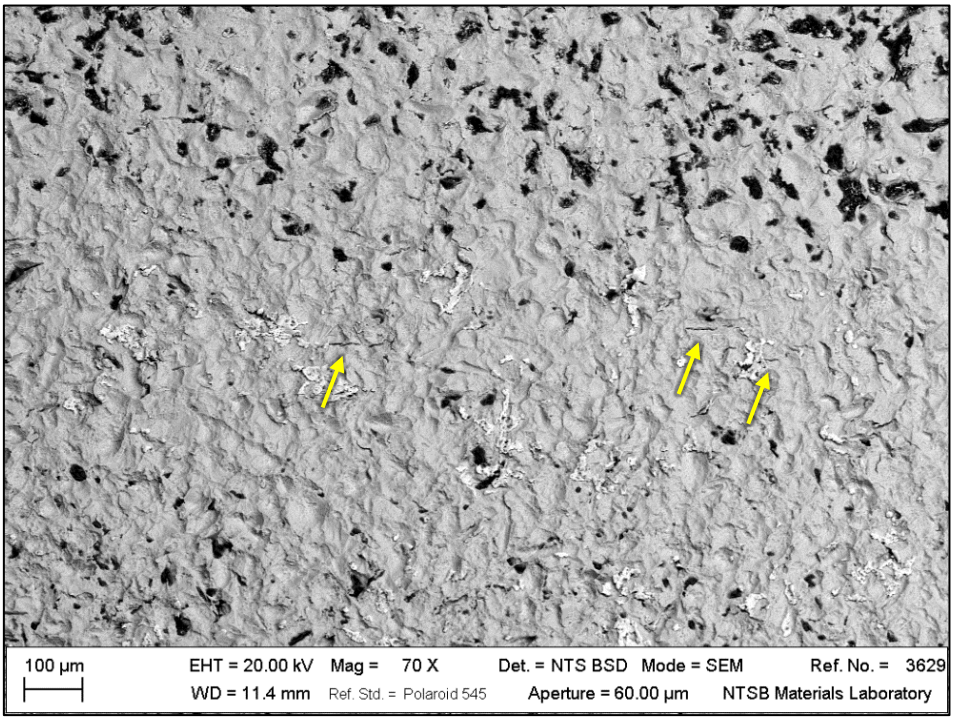

Figure 19. SEM image using the backscattered electron detector showing the etched surface of blade 20. Unlabeled arrows indicate isolated microcracks.

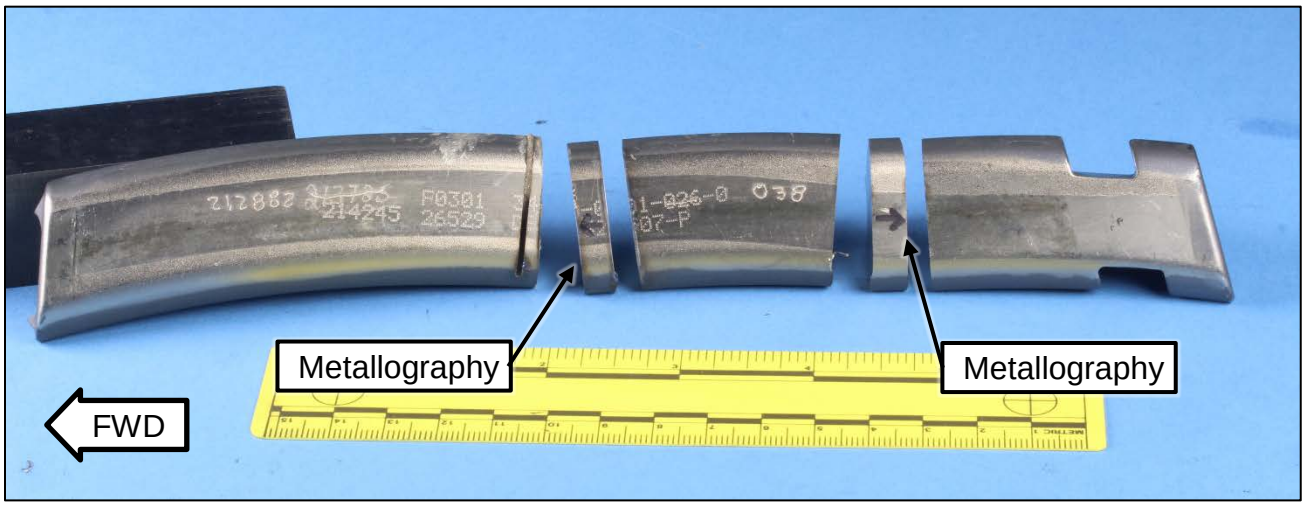

Figure 20. Overall view of the blade 13 piece sectioned for metallography on the faces indicated.

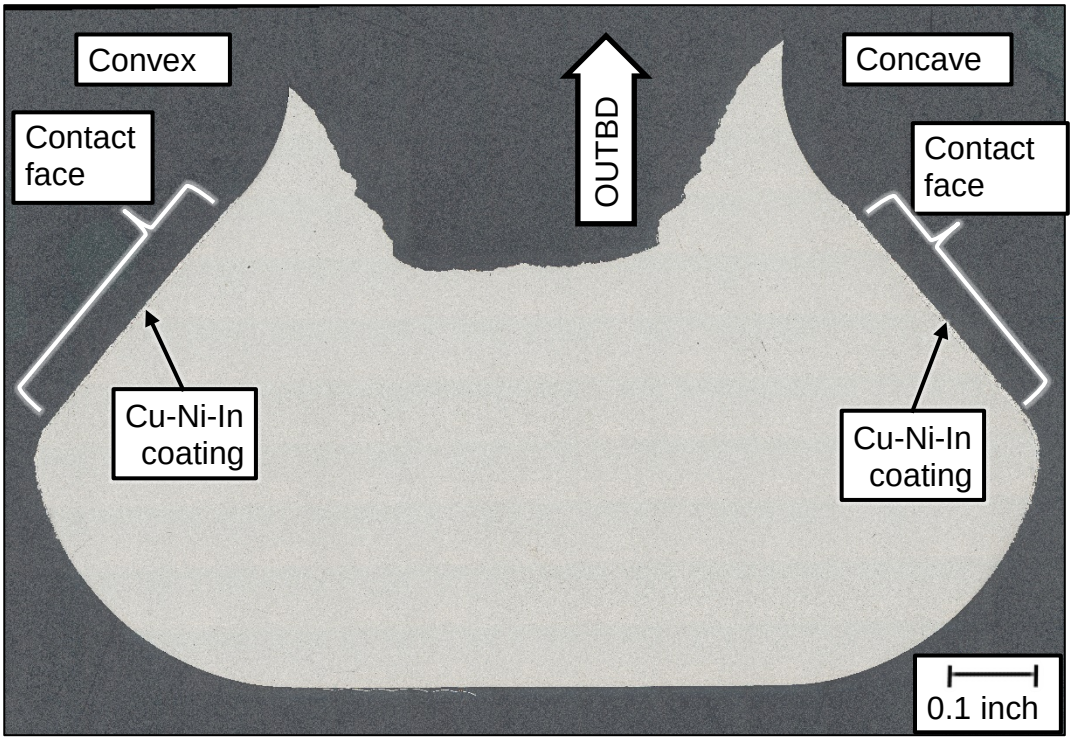

Figure 21. Macrograph showing the as-polished transverse plane through the dovetail near the middle of the axial length of the dovetail.

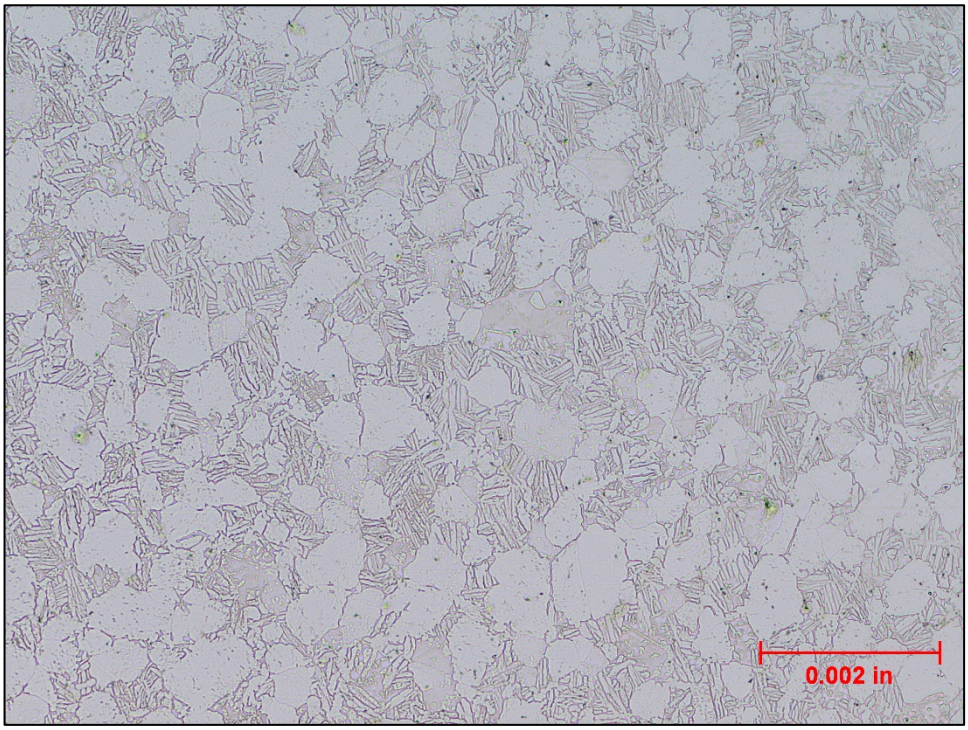

Figure 22. Typical etched microstructure in the blade 13 dovetail. (Etched with Kroll's reagent.)

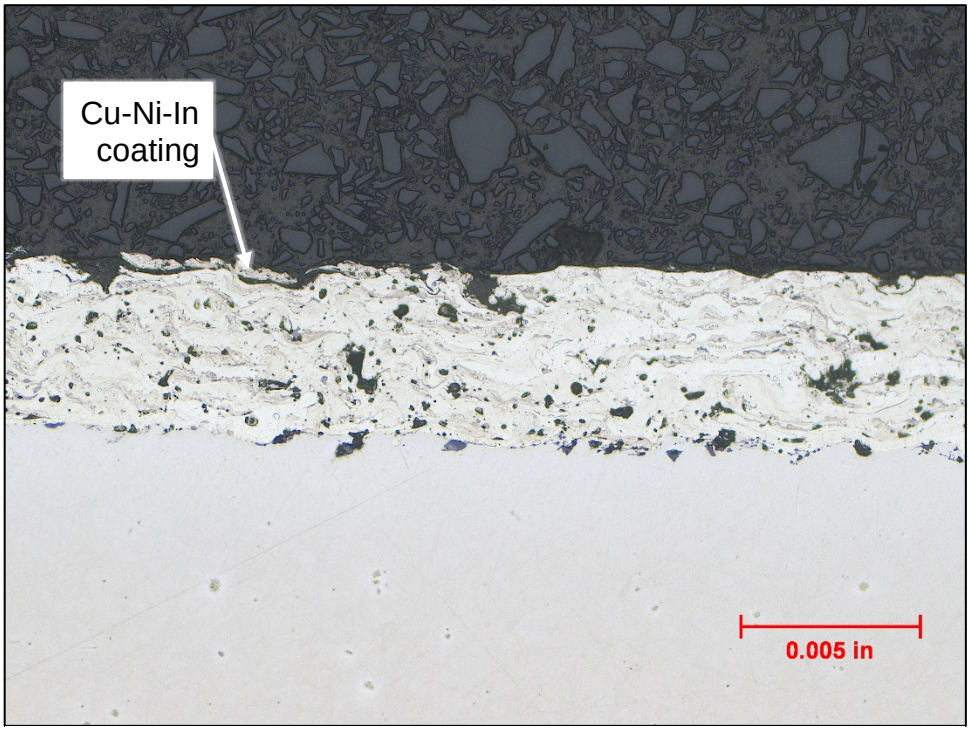

Figure 23. Micrograph of the Cu-Ni-In coating near the middle of the contact face on the convex side of the cross-section shown in the previous figure.

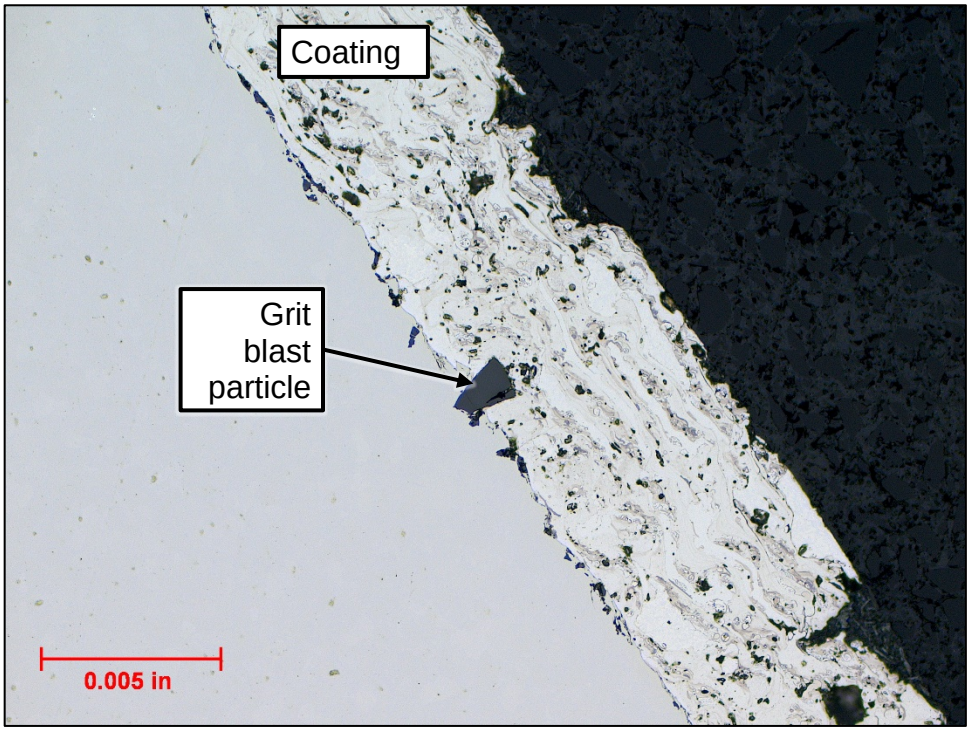

Figure 24. Concave side of the coating showing a relatively large grit-blast particle embedded in the surface.

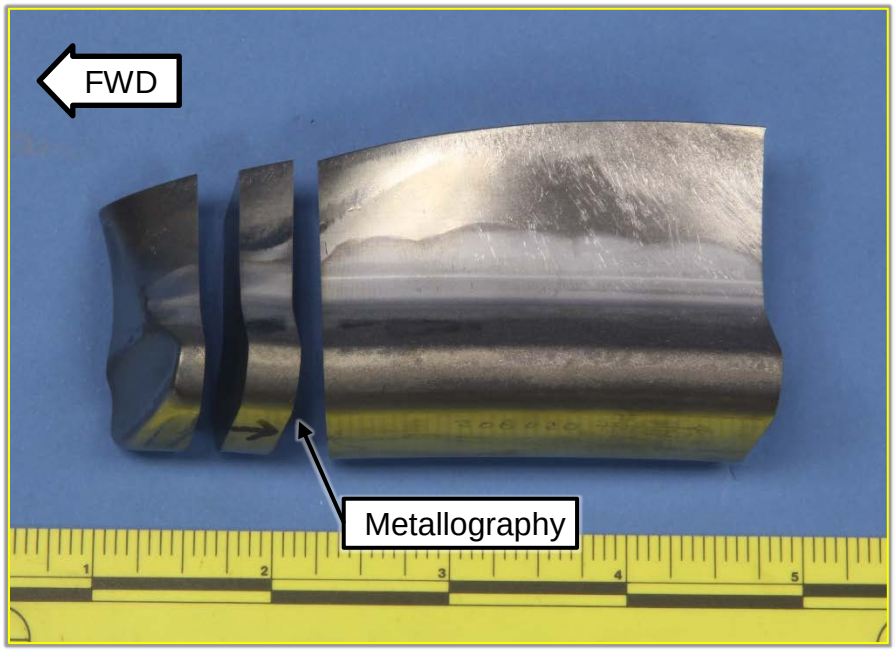

Figure 25. Overall view of the blade 20 piece sectioned for metallography on the face indicated.

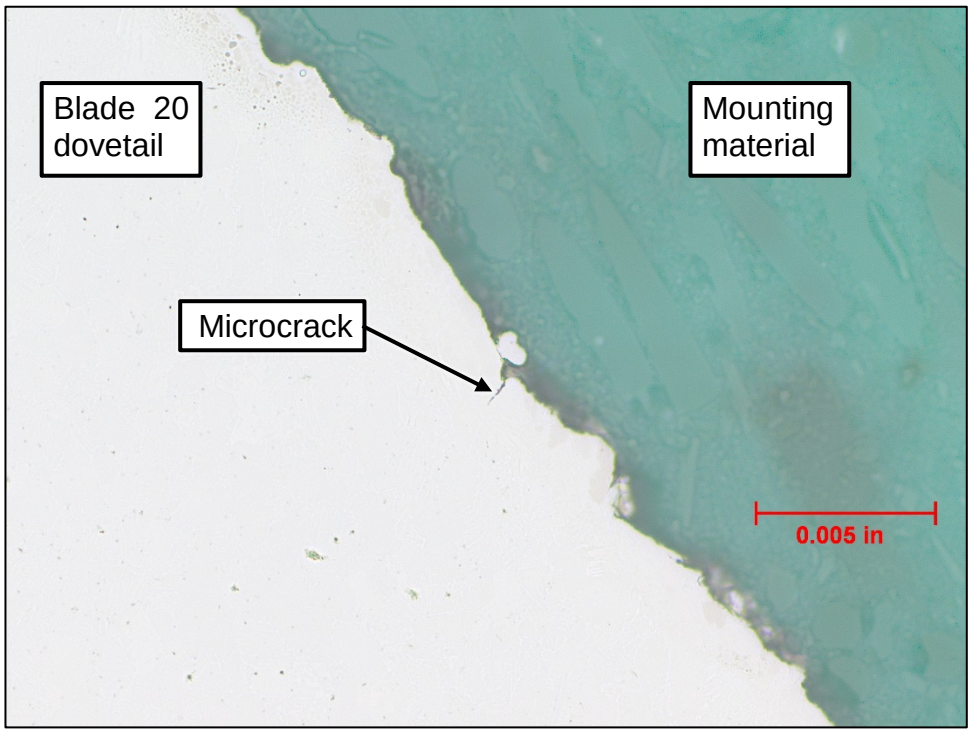

Figure 26. Microcrack in the grit-blast region of the convex face in the as-polished cross-section of blade 20 in the transverse plane shown in the previous figure.

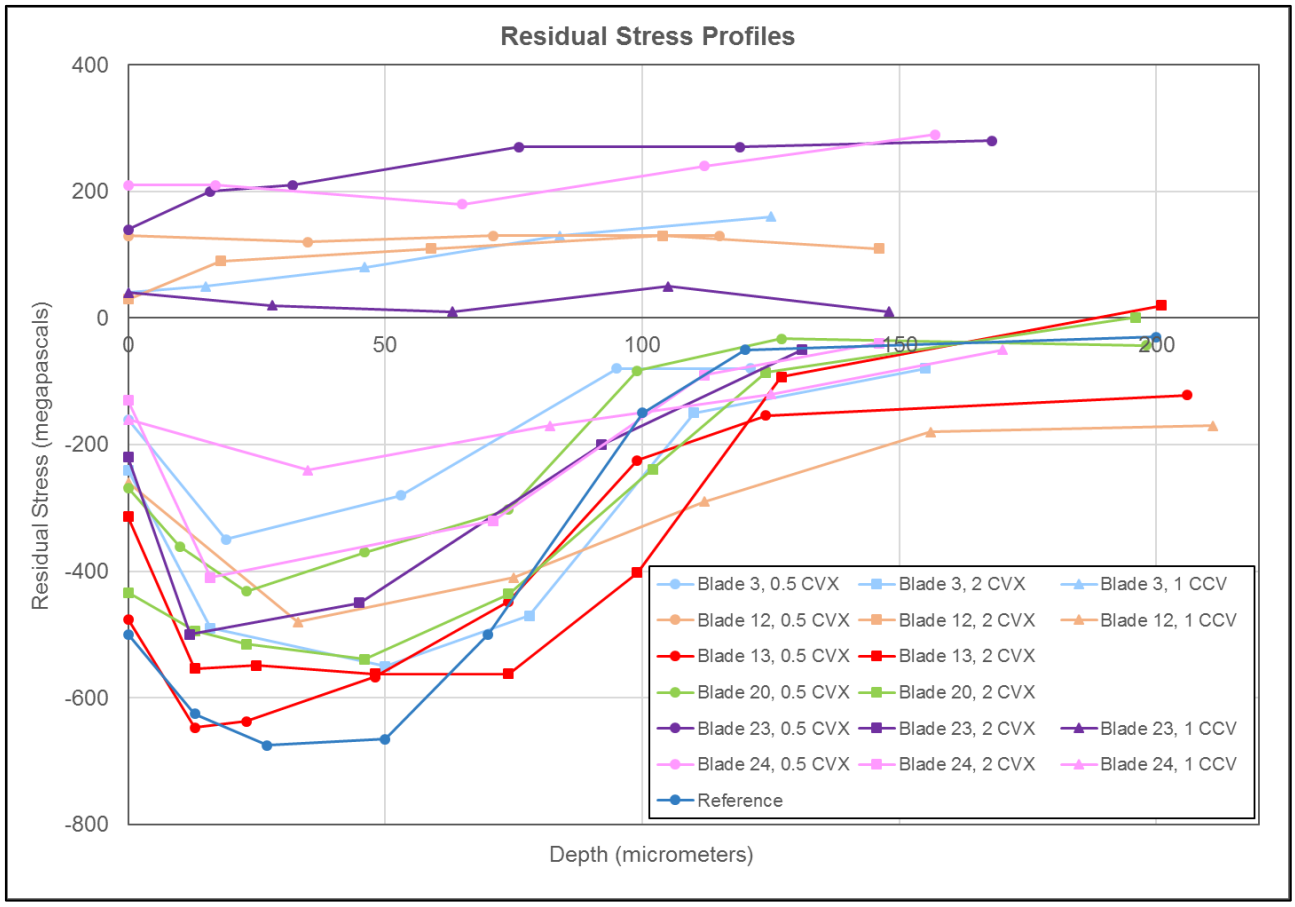

Figure 27. Residual stress profiles for fractured blade 13 and intact blades 3, 12, 20, 23, and 24. In the legend, identifiers 0.5 CVX, 2 CVX, and 1 CCV after the blade number indicate measurement locations with distance in inches from the leading edge on the convex (CVX) side or from the trailing edge slot on the concave (CCV) side. The reference residual stress profile is also shown for comparison.

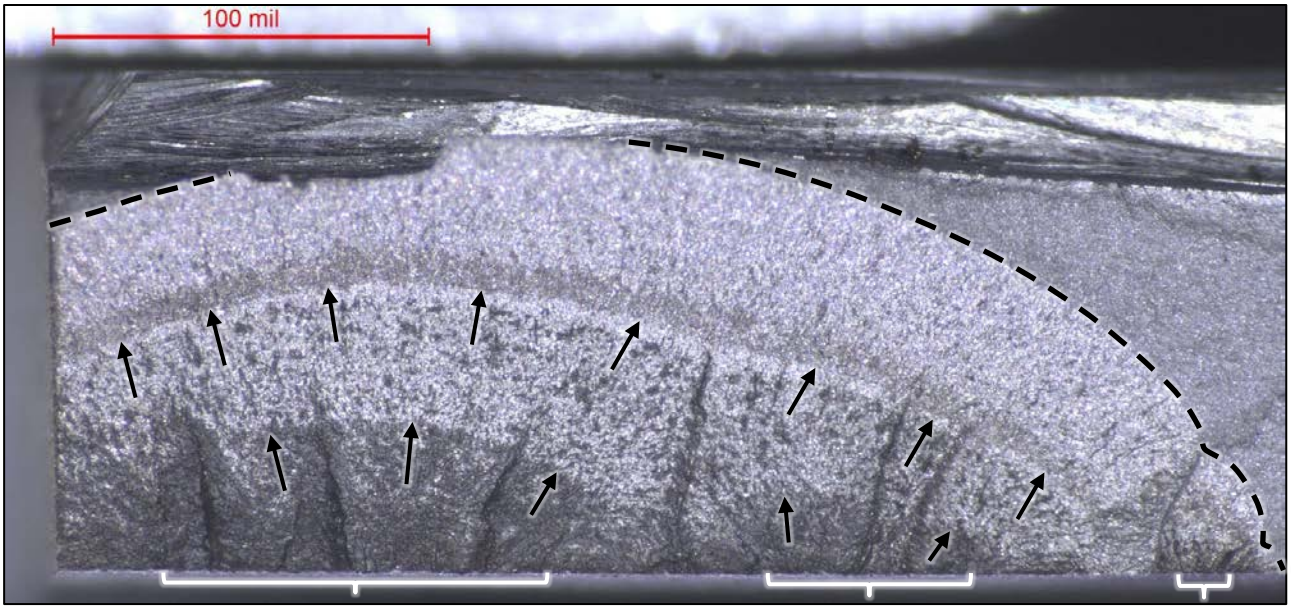

Figure 28. Overall view of the crack fracture surface of blade M after opening by lab fracture. Dashed lines indicate the crack boundary. Unlabeled brackets and arrows indicate the location of fatigue origins and crack arrest lines, respectively. Photo courtesy of GE Aviation.

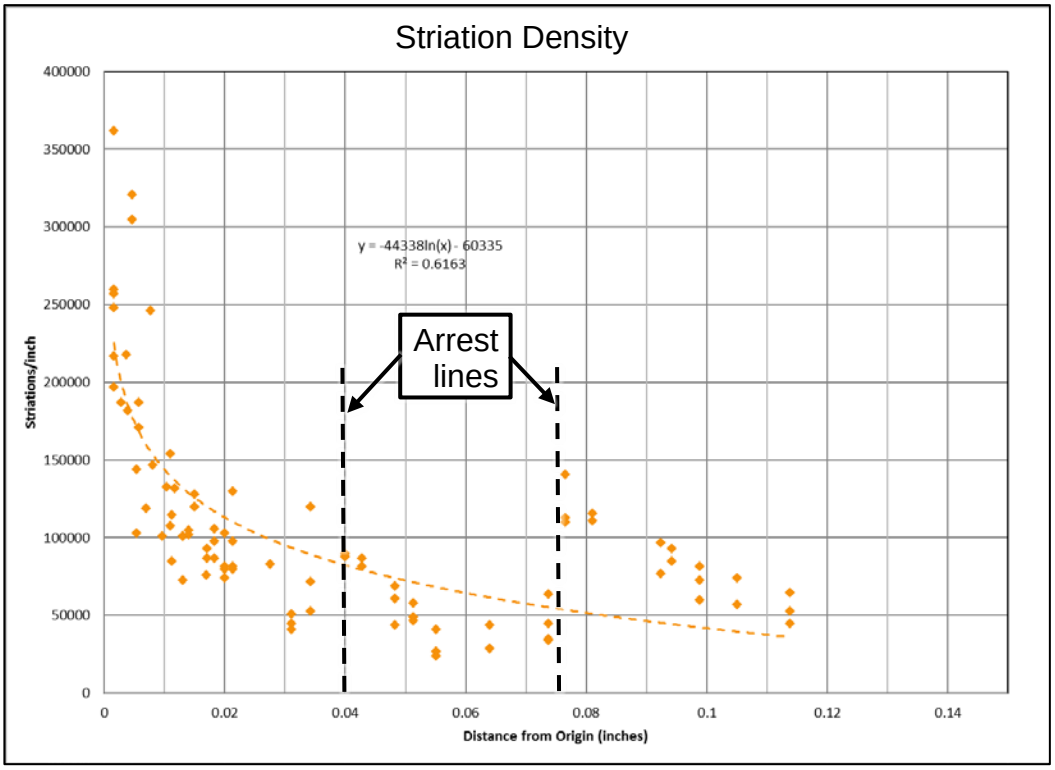

Figure 29. Striation density as a function of distance from the origin for blade M. Locations of crack arrest lines are noted on the graph. Data acquired by GE Aviation.

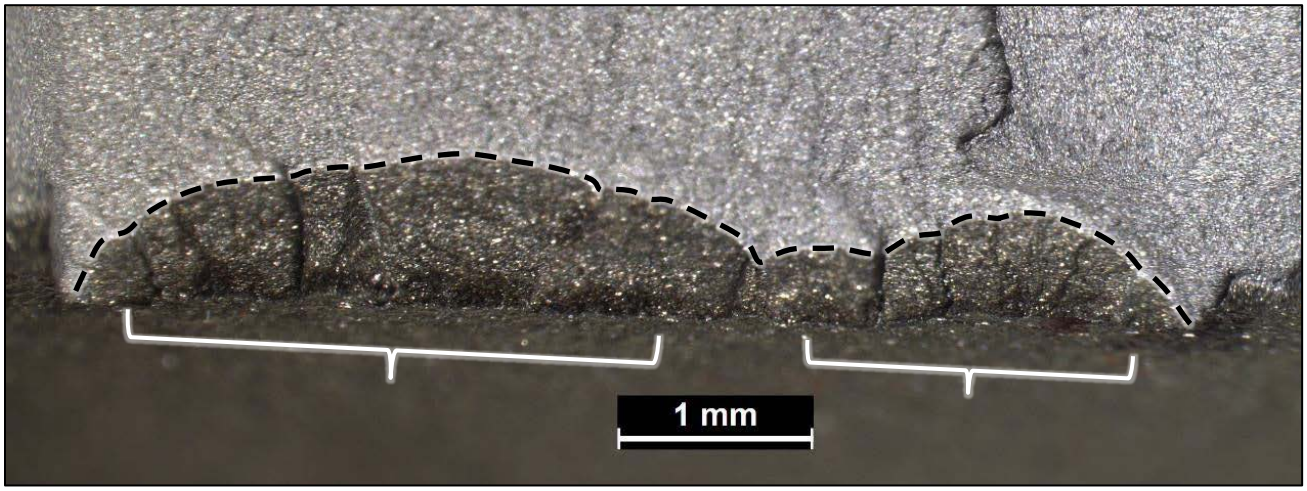

Figure 30. Overall view of the crack fracture surface of blade N after opening by lab fracture. Dashed lines indicate the crack boundary. Unlabeled brackets indicate the location of fatigue origins. Photo courtesy of Safran Aircraft Engines.

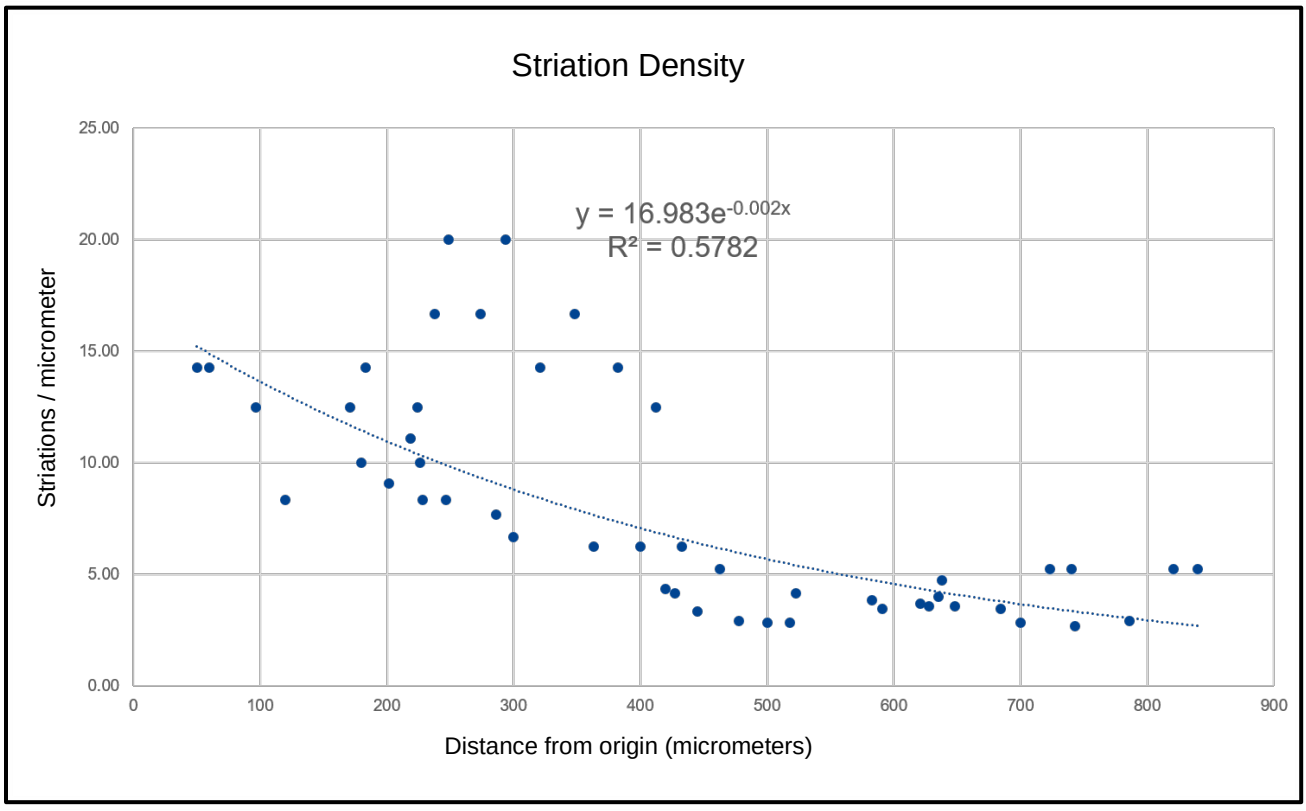

Figure 31. Striation density as a function of distance from the origin for blade N. Data acquired by Safran Aircraft Engines.

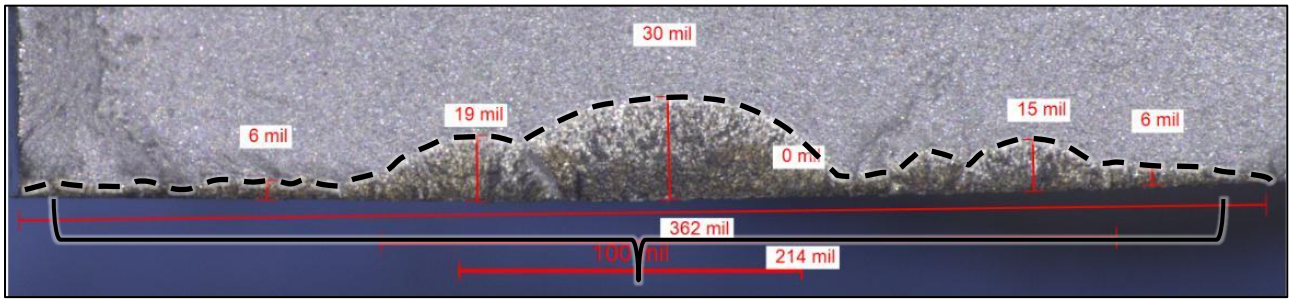

Figure 32. Overall view of the crack fracture surface of blade O after opening by lab fracture. A dashed line indicates the crack boundary, and an unlabeled bracket indicates the location of fatigue origins. Photo courtesy of GE Aviation.

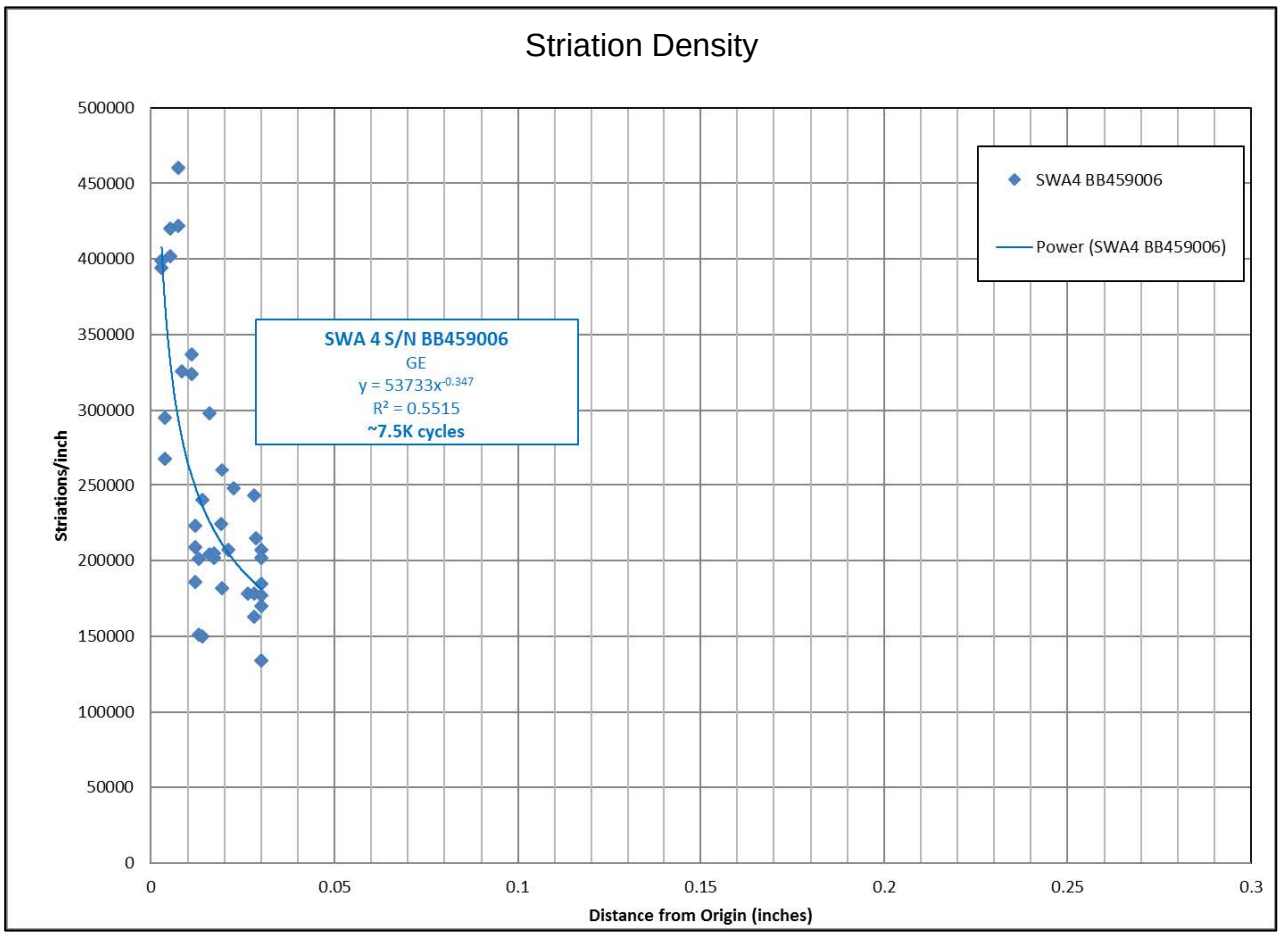

Figure 33. Striation density as a function of distance from the origin for blade O. Data acquired by GE Aviation.

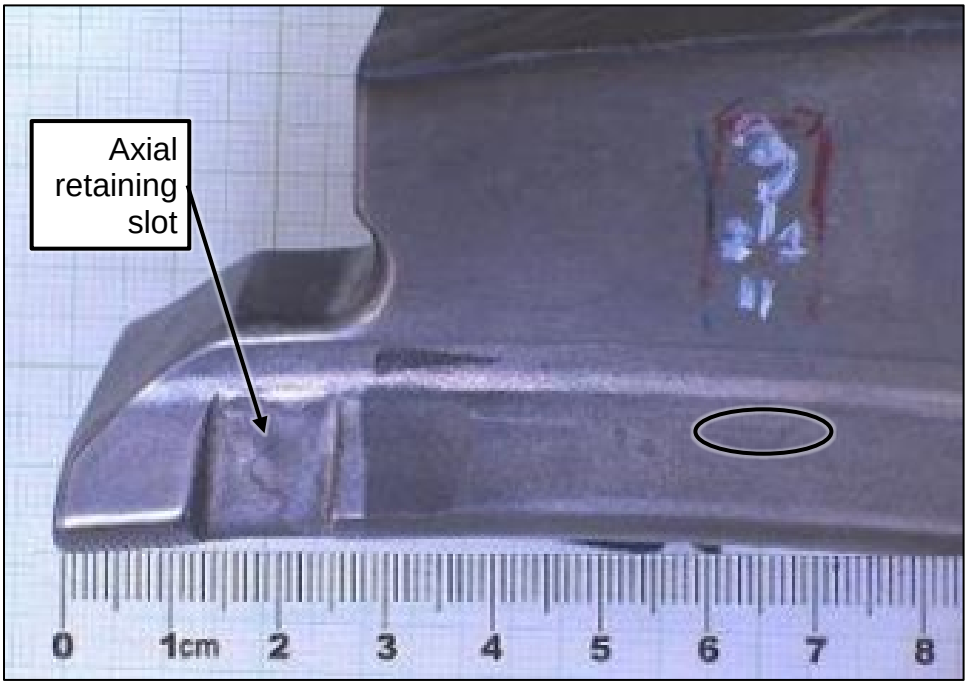

Figure 34. Crack location (circled area) near the aft end of blade P on the concave side contact face. Photo courtesy of Safran Aircraft Engines.

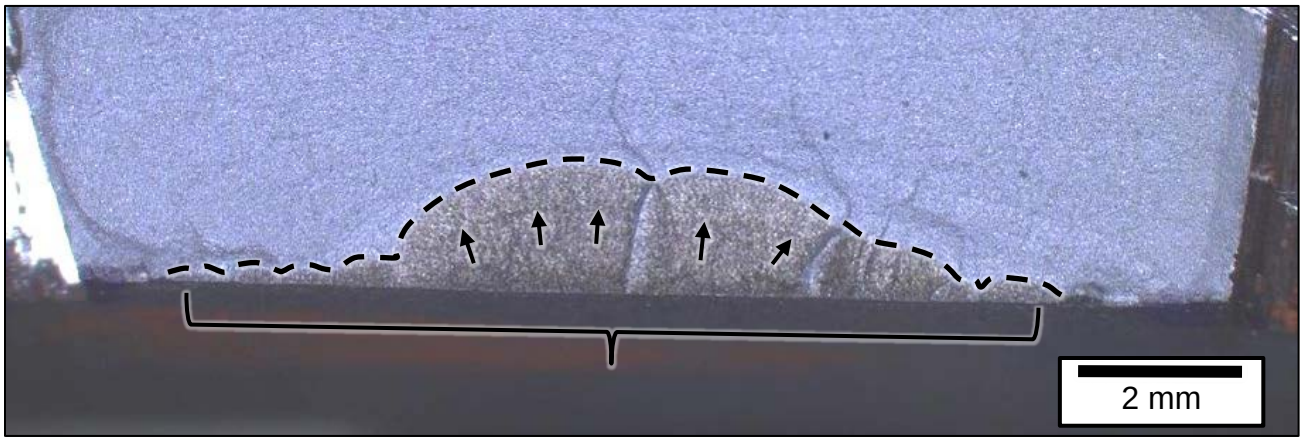

Figure 35. Overall view of the crack fracture surface of blade P after opening by lab fracture. Dashed lines indicate the crack boundary. Unlabeled brackets and arrows indicate the location of fatigue origins and crack arrest lines, respectively. Photo courtesy of Safran Aircraft Engines.

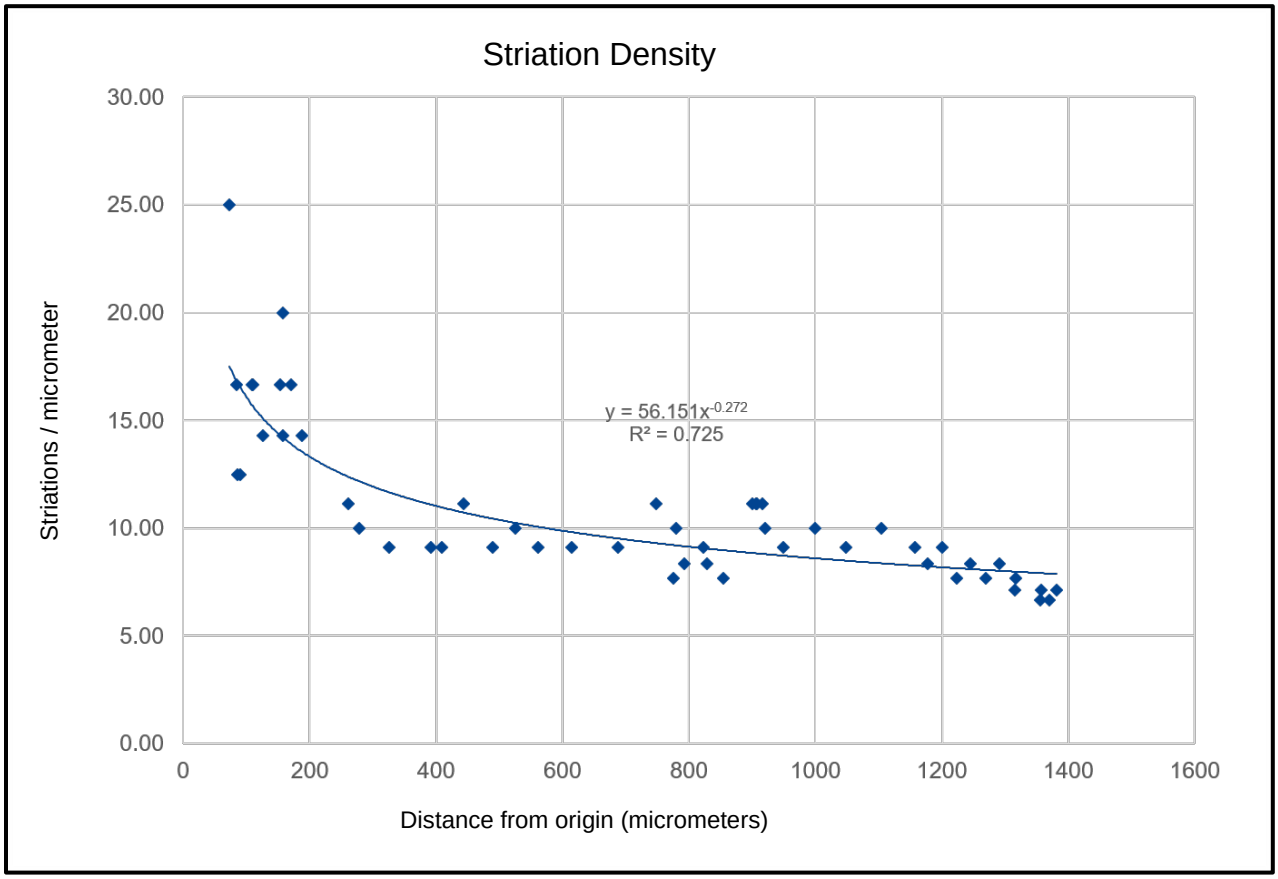

Figure 36. Striation density as a function of distance from the origin for blade P. Data acquired by Safran Aircraft Engines.